Genetics: Published Articles Ahead of Print, published on June 4, 2006 as 10.1534/genetics.106.057836

The F-box protein Dia2 overcomes replication impedance to promote genome stability in *Saccharomyces cerevisiae*

Deborah Blake[*,†], Brian Luke[‡,1], Pamela Kanellis[*,†], Paul Jorgensen[†,2], Theo Goh[†,3], Sonya Penfold[†,4], Bobby-Joe Breitkreutz[†], Daniel Durocher[*,†], Matthias Peter[‡] and Mike Tyers[*,†]

[*]Department of Medical Genetics and Microbiology, University of Toronto, Toronto, Ontario, Canada M5S 1A8

[†]Samuel Lunenfeld Research Institute, Toronto, Ontario, Canada M5G 1X5

[‡]Institute of Biochemistry, HPM G 10.0, ETH Hönggerberg 8093 Zürich Switzerland

[1]Present Address: Swiss Institute for Cancer Research, ISREC, 1066 Epalinges

[2]Present Address: Department of Systems Biology, Harvard Medical School, Boston, MA, 02115

[3]Present Address: Ontario Cancer Institute and Campbell Family Institute for Breast Cancer Research, Toronto, Ontario, Canada M5G 2C1

[4]Present Address: TM Bioscience Corporation, Toronto, Ontario, Canada M5G 1Y8

Running title:

Dia2 promotes genome stability

Keywords:

DNA damage, chromosome loss, rDNA, SCF ubiquitin ligase, SGA

Corresponding Author:

Mike Tyers

Samuel Lunenfeld Research Institute, Mount Sinai Hospital

Room 1080, 600 University Avenue

Toronto, Ontario

Canada

M5G 1X5

Phone: (416) 586-8371

Fax: (416) 586-8869

e-mail: tyers@mshri.on.ca

ABSTRACT

The maintenance of DNA replication fork stability under conditions of DNA damage and at natural replication pause sites is essential for genome stability. Here, we describe a novel role for the F-box protein Dia2 in promoting genome stability in the budding yeast *Saccharomyces cerevisiae*. Like most other F-box proteins, Dia2 forms an SCF (Skp1-Cdc53/Cullin-F-box) E3 ubiquitin ligase complex. Systematic analysis of genetic interactions between *dia2Δ* and ~4,400 viable gene deletion mutants revealed synthetic lethal/synthetic sick interactions with a broad spectrum of DNA replication, recombination, checkpoint, and chromatin remodeling pathways. *dia2Δ* strains exhibit constitutive activation of the checkpoint kinase Rad53 and elevated counts of endogenous DNA repair foci, and are unable to overcome MMS-induced replicative stress. Notably, *dia2Δ* strains display a high rate of gross chromosomal rearrangements (GCRs) that involve the rDNA locus and an increase in extra-chromosomal rDNA circle (ERC) formation, consistent with an observed enrichment of Dia2 in the nucleolus. These results suggest that Dia2 is essential for stable passage of replication forks through regions of damaged DNA and natural fragile regions, particularly the replication fork barrier (RFB) of rDNA repeat loci. We propose that the SCF^{Dia2} ubiquitin ligase serves to modify or degrade protein substrates that would otherwise impede the replication fork in problematic regions of the genome.

INTRODUCTION

Faithful DNA replication requires the stabilization of replication forks at natural pause sites and at sites of DNA damage (BRANZEI and FOIANI 2005). Collapse of replication forks results in the formation of DNA double-strand breaks (DSBs) that can then lead to illegitimate recombination and genome rearrangements, both of which are thought to be underlying causes of many human cancers (LENGAUER *et al.* 1998). Physical impediments to replication fork progression include tightly bound non-nucleosomal protein-DNA complexes, DNA secondary structures and regions of DNA damage, whereas inadequate dNTP pools cause forks to slow and eventually stall in a non-locus specific manner (BRANZEI and FOIANI 2005). Accumulated DNA damage or stalled replication forks elicit a checkpoint response that results in a delay of the cell cycle, induction of damage responsive genes, and the repair or bypass of the DNA lesion (MELO and TOCZYSKI 2002; BRANZEI and FOIANI 2005). The DNA damage checkpoint is activated upon detection of DNA lesions in G1 and G2 phase, and also in S phase, the latter sometimes being referred to as the intra-S checkpoint. A second response in S phase, referred to as the replication checkpoint, responds to delayed DNA synthesis, as caused by lowered dNTP pools upon inhibition of ribonucleotide reductase by hydroxyurea (HU). It is likely that the replication and intra-S checkpoint pathways are integrated such that the key signal is stalled or slowed replication forks, due to either dNTP shortage or collision with DNA damage. The only essential function of the S-phase checkpoint is to stabilize the fork when cells undergo replicative stress (TERCERO *et al.* 2003) and thereby prevent the accumulation of recombinogenic structures (LOPES *et al.* 2001).

In both eukaryotic and prokaryotic genomes, region-specific barriers to replication fork progression pause and maintain replication forks in problematic regions of the genome (ROTHSTEIN *et al.* 2000). In budding yeast, replication pause sites have been characterized at rDNA repeats, centromeres, *tRNA* genes, inactive origins, silent mating type loci, telomeres, and other delimited regions along the length of chromosome III (BREWER and FANGMAN 1988; GREENFEDER and NEWLON 1992; CHA and KLECKNER 2002; IVESSA *et al.* 2002). These sites are likely formed by stable protein complexes, which may either be incidental or may help coordinate various cellular processes with DNA replication. In particular, a high rate of transcription impairs replication fork progression and causes transcription-associated recombination (TAR), a phenomenon that occurs at both natural loci such as the rDNA repeats and tRNA genes, and also at artificially-induced high level transcription zones (DESHPANDE and NEWLON 1996; IVESSA *et al.* 2003; PRADO and AGUILERA 2005).The best characterized pause site is the replication fork barrier (RFB) that resides in the rDNA repeats (BREWER and FANGMAN 1988). The RFB establishes a polar block to replication, i.e., DNA polymerase pauses only in the direction that is convergent to transcription, and is thus thought to coordinate the high rate of rDNA transcription with replication of the rDNA locus (KOBAYASHI *et al.* 1998; TAKEUCHI *et al.* 2003). RFB activity depends on Fob1, which binds a discreet sequence in the non-transcribed spacer of the rDNA repeat, and is necessary for elevated rates of recombination at the rDNA locus, including extra-ribosomal rDNA circle (ERC) formation (KOBAYASHI 2003). Programmed pause sites appear to be a ubiquitous feature of the replication process; for example, polar replication barriers have been identified in bacteria (PAI *et al.* 1996).

When a block to replication cannot be overcome, the S-phase checkpoint machinery promotes replication fork stabilization and subsequent restart (BRANZEI and FOIANI 2005). If this mechanism fails, ensuing fork collapse results in dissociation of the replisome and the generation of replication intermediates including DSBs (CHA and KLECKNER 2002; SOGO *et al.* 2002; COTTA-RAMUSINO *et al.* 2005). To resume replication, recombination proteins are recruited to sites of collapsed forks, thus permitting homologous recombination pathways to aid in the bypass of the DNA lesion (LAMBERT *et al.* 2005). While recombination in this circumstance promotes cell viability, it comes at the expense of an increase in intra- and inter-chromosomal recombination that leads to site-specific gross chromosomal rearrangements (GCRs) (LAMBERT *et al.* 2005). Recombination-mediated replication restart is thus a means of last resort to rescue a collapsed fork and is for this reason actively suppressed. Several parallel pathways inhibit or resolve recombination events at the replication fork, including the Sgs1 and Srs2 DNA helicases (BRANZEI and FOIANI 2005; CHANG *et al.* 2005; LIBERI *et al.* 2005; MULLEN *et al.* 2005). The replication machinery can also circumscribe regions of damaged DNA, either by fork reversal and template switching to the sister chromatid strand or through recruitment of specialized translesion synthesis DNA polymerases, as controlled by modified forms of the processivity factor PCNA/Pol30 (BRANZEI and FOIANI 2005).

The ubiquitin-proteasome system targets many regulatory proteins for rapid intracellular proteolysis (HERSHKO 1983). Ubiquitin is conjugated to target proteins by a step-wise cascade of E1, E2 and E3 enzymes, which activate and transfer ubiquitin as a thioester linkage for ultimate transfer to a lysine residue on the substrate. Reiteration of

the catalytic cycle synthesizes a ubiquitin polymer that targets the substrate to the 26S proteasome, where it is rapidly unfolded and degraded. A diverse array of E3 enzymes, often also referred to as ubiquitin ligases, specifically recognize one or more cognate substrates. Ubiquitin ligases fall into general classes: the HECT domain class, which forms a catalytic thioester with ubiquitin for transfer to the bound substrate, and the RING domain class, which bind and juxtapose both the E2 and the substrate (PICKART 2001). The archetypal and best characterized of RING domain ubiquitin ligases are the Skp1-Cdc53/Cullin-F-box (SCF) family. SCF complexes are composed of the linker protein Skp1, the cullin scaffold protein Cdc53 and the RING domain protein Rbx1/Roc1/Hrt1 and any one of a number of variable substrate recognition subunits called F-box proteins (BAI *et al.* 1996; PATTON *et al.* 1998). F-box proteins contain a Skp1 binding site called the F-box and a substrate interaction domain, such as a WD40 repeat domain or a leucine rich repeat (LRR) domain, which often recognize substrates in a phosphorylation-dependent manner (WILLEMS *et al.* 2004). Budding yeast contains 21 recognizable F-box proteins, but as yet only a few of these have well characterized functions.

We describe a novel role for the F-box protein Dia2 in maintaining genome stability. *DIA2* was initially identified in a screen for mutants that exhibit increased invasive growth, although *dia2Δ* strains are only weakly invasive (PALECEK *et al.* 2000). It has been suggested that Dia2 mediates the degradation of Tec1, a transcription factor implicated in invasive growth (BAO *et al.* 2004), and of ectopically expressed human cyclin E (KOEPP *et al.* 2001); however, it is likely that the actual F-box protein for both of these substrates is Cdc4 (KOEPP *et al.* 2001; CHOU *et al.* 2004).The function of Dia2

thus remains equivocal. Here, we report that the *dia2Δ* mutation exhibits synthetic lethal/sick interactions with a host of replication and repair mutations, as well as sensitivity to DNA damaging agents. Concordant with these genetic interactions, *dia2Δ* strains are defective in S-phase progression, have a high rate of endogenous DNA damage and constitutively activate the DNA damage checkpoint. Moreover, the rates of chromosome loss, GCRs and extra-chromosomal rDNA circle (ERC) formation are highly elevated in the *dia2Δ* mutant. These *dia2Δ* phenotypes suggest that Dia2 normally enables the replication machinery to cope with both extrinsically damaged DNA templates and intrinsic replication barriers and that in the absence of Dia2, accumulation of endogenous damage results from the collapse of replication forks. SCF^{Dia2} likely mediates degradation or modification of one or more substrates that would otherwise interfere with replication fork stability in problematic regions of the genome.

MATERIALS AND METHODS

Strains and growth conditions: Strains used in this study were constructed by standard methods and are described in Table 1. Except where specified, cultures were grown in rich XY medium (2% peptone, 1% yeast extract, 0.01% adenine, 0.02% tryptophan) containing 2% glucose. Cell size was determined essentially as described (JORGENSEN *et al.* 2004) using a Coulter Channelizer Z2 (Beckman-Coulter). Cells were synchronized in G1 phase in the presence of 5 μg/ml alpha-factor for 2 h at 30°. An *RNR*1-expressing plasmid (pMT2581) was used to ensure viability of *mrc1Δ rad9Δ* double mutants derived from genetic crosses.

FACS analysis: Approximately 1 x 10^7 cells were collected from log phase cultures and processed as described (JORGENSEN *et al.* 2004). DNA was stained with Sytox Green (Molecular Probes) and profiles analyzed using a Becton Dickinson FACS Calibur machine and the CellQuest Pro and ModFit LT software (BD Biosciences).

DNA damage and genotoxic stress assays: Saturated cultures were adjusted to OD_{600} = 0.8, serially diluted in ten-fold steps and 4 µL volumes spotted onto untreated medium or medium containing or exposed to 0.02% (v/v) MMS, 200 mM HU, 5 µg/mL camptothecin, 0.1 µg/mL 4-NQO, 200 J/M^2 UV or 100 grays X-rays. Plates were incubated at 30° for 2 days. Conditions used to test for the intra-S checkpoint were as described (PAULOVICH and HARTWELL 1995). Plasmids expressing full length *DIA2* (pMT2484) or *DIA2*$^{\Delta F\text{-}box}$ (pMT2742) from the endogenous *DIA2* promoter were used in MMS sensitivity complementation tests.

Protein detection: Co-immunoprecipitation experiments with FLAG- and MYC- tagged constructs were as described previously (HO *et al.* 2002). For immunoblots, proteins were separated on a 10% or 12% SDS-PAGE, transferred to PVDF membranes and probed with 9E10 monoclonal antibody (1:10,000), anti-FLAG M2 monoclonal antibody (1:2,000, Sigma) or anti-Skp1 polyclonal (1:5,000), as indicated. Detection was with HRP conjugated secondary antibodies at 1:10,000 dilution (Amersham) followed by Supersignal West Pico chemiluminescent substrate (Pierce) and analysis on a Fluor-S Multiimager (Biorad). To detect Rad53 isoforms, log phase cultures were arrested in G1 phase with alpha-factor, washed and released into fresh media. Total protein extracts were resolved by 7.5% SDS-PAGE, transferred onto nitrocellulose and probed with a primary rabbit anti-Rad53 antibody (1:750) and secondary donkey anti-rabbit HRP

conjugated antibody (1:10,000, Amersham). For in situ autophosphorylation (ISA) assays, log phase cultures were either treated or not with 200 mM HU for one hour, then processed as described (PELLICIOLI *et al.* 1999).

Synthetic genetic array (SGA) screen: A *dia2Δ::URA3 MATα* strain (yMT1940) was mated to a collection of 4,422 individual *xxx::kanR MATa* haploid deletion mutants (GIAEVER *et al.* 2002) by manual replica pinning as described (TONG *et al.* 2001). Three independent screens were carried out in triplicate. All genetic interactions identified in at least two of the three screens were subsequently confirmed by tetrad analysis. Synthetic lethal interactions were defined as double mutants that failed to grow either in the original tetrad or upon re-streaking onto fresh medium; synthetic sick interactions were defined as double mutants that grew noticeably more slowly than either single gene deletion strain. Two-dimensional hierarchical clustering of *dia2Δ* synthetic genetic interactions was performed against a dataset of 284 SGA and dSLAM screens (TONG *et al.* 2004; PAN *et al.* 2006; REGULY *et al.* 2006) using an average linkage clustering algorithm (EISEN *et al.* 1998) and MapleTree (http://mapletree.sourceforge.net/). Graphical representations of genetic interactions were rendered with the Osprey visualization suite (BREITKREUTZ *et al.* 2003). All data are available from the BioGRID interaction database at http://www.thebiogrid.org (STARK *et al.* 2006).

Microarray analysis: Genome-wide expression profiles were determined for *dia2Δ* (yMT2078) and isogenic wild-type (yMT1448) strains grown to early log phase (OD 0.2-0.4) at 30°. Polyadenylated RNA was fluorescently labeled with Cy3 or Cy5 conjugated dCTP (Amersham) and *dia2Δ* and wild-type samples competitively hybridized against full genome 6,200 feature ORF arrays (UHN Microarray Centre, Toronto). All

hybridizations were replicated with fluor reversal. Arrays were scanned with a Scanarray 4000 (GSI Lumonics) and images processed by eliminating corrupted spots, normalizing spot intensity to total Cy5 and Cy3 signal, eliminating spots with low intensity, and averaging duplicate spots (JORGENSEN *et al.* 2004).

Genome instability assays: Chromosome loss rate of a *CFIII-SUP11-HIS* reporter fragment was measured as described (HIETER *et al.* 1985). After growth to saturation overnight in SD-trp -his 2% glucose medium to maintain the artificial chromosome, cells were diluted into SD- trp 2% glucose media, grown for 6 hrs at 30º to early log phase (2-4 x 10^6 cells/mL), sonicated briefly, and plated on SD-trp -ade 2% glucose agar media supplemented with a limited amount of adenine (10mg/L). Chromosome loss rate per generation was calculated as the number of half- sectored colonies divided by the number of colonies. GCR rates were determined with a strain in which *HXT13* (~7.5 kb telomeric to *CAN1* on *Chr V*) is replaced by *URA3* (CHEN and KOLODNER 1999). Control (yMT3420) and *dia2Δ* (yMT3812) revertants that arose from loss of the region encompassing *CAN1* and *URA3* were scored on canavanine and 5-FOA containing medium. Rates were calculated by fluctuation analysis using the method of the median as described (KANELLIS *et al.* 2003), and represent the average of two independent experiments using sets of five independent cultures. Mitotic recombination rates were determined by loss of an *ADE2* marker integrated into the rDNA locus on *Chr XII* as described (CHRISTMAN *et al.* 1988). Recombination rate per generation was calculated by dividing the number of half-sectored colonies by the total number of colonies.

Pulse field gel electrophoresis (PFGE) and hybridization: Standard PFGE procedures were used according to the manufacturer's instructions (Bio-Rad, Hercules,

Calif.). Agarose plugs containing 3 x 10^8 cells/mL were loaded onto a 1% agarose gel in 0.5 x Tris-borate EDTA (TBE) buffer and electrophoresed at 6V at an angle of 120° for 24 h at 14° with an initial switch time of 60 seconds and a final switch time of 120 seconds. Gels were stained and photographed, then transferred to nylon membranes and probed with [^{32}P] -γ-ATP-labeled *35S* rDNA or *MCM3* fragments. To assess formation of ERCs, plugs were prepared as above and DNA resolved on a conventional 1% agarose gel. Gels were transferred to nylon membranes and probed with a [^{32}P] -γ-ATP-labeled *35S* rDNA fragment.

Live cell imaging and fluorescent microscopy: DIC and fluorescence microscopy were performed with an Eclipse E600FN microscope (Nikon) and Orca CCD camera (Hamamatsu). Metamorph Software (Universal Imaging) was used to capture and process images as described (JORGENSEN *et al.* 2004). YFP exposure times were in the range of 150-200 ms and serial sections through live cells were set to 21 z-planes at 0.4μm spacing.

RESULTS

Absence of Dia2 causes an S/G2/M cell cycle delay: Unlike most F-box proteins that contain a single C-terminal protein interaction domain, Dia2 is unusual in that it contains an N-terminal tetratricopeptide repeat (TPR) domain and a C-terminal LRR domain (WILLEMS *et al.* 2004). As not all F-box proteins form SCF complexes (WILLEMS *et al.* 2004), we assessed whether Dia2 assembled into an SCF complex in vivo (Figure 1A). An interaction was detected between Dia2 and the SCF core subunits Cdc53 and Skp1, in accord with the previously reported in vitro reconstitution of SCF^{Dia2} (KOEPP *et al.*

2001; KUS *et al.* 2004). Strains that lacked *DIA2* grew at a rate 30% slower than wild-type cells and exhibited a heterogeneous colony size (Figure 1B). The small sized colonies were not due to petite formation caused by loss of mitochondrial DNA because all colonies were able to grow anerobically on glycerol medium (data not shown). Intriguingly, *dia2Δ* strains developed an increasingly severe growth defect upon prolonged propagation (data not shown). Asynchronous populations of *dia2Δ* strains had a modal cell size that was twice that of wild-type strains (Figure 1C). The slow growth rate and increased cell size suggested a defect in cell cycle progression, and consistently, FACS analysis of DNA content revealed an accumulation of cells in both S and G2/M phase (Figure 1D). The absence of Dia2 thus resulted in an S/G2/M cell cycle delay, which in other contexts often results from S phase defects that activate the G2/M cell cycle checkpoint.

Genetic interactions of *DIA2* with DNA replication, repair and checkpoint pathways: To delineate Dia2 function, we employed synthetic genetic array (SGA) technology to construct a collection of double mutants between *dia2Δ* and an ordered array of 4,422 viable single gene deletion strains (TONG *et al.* 2001). Double mutant combinations that result in inviability (synthetic lethality, SL) or reduced fitness (synthetic sickness, SS) identify genes that either converge on an essential biological process or that exhibit a damage-response relationship (HARTMAN *et al.* 2001). The SGA screen identified 55 deletion mutants that exhibited overt synthetic genetic interactions with *dia2Δ,* all of which were confirmed by tetrad analysis. 19 of the 55 double mutant interactions were synthetic lethal (Figure 2). Many of the interactions occurred with genes implicated in DNA replication (e.g., *RRM3, PIF1, RAD27, RNR4*), recombination

(e.g., *RAD52, MRE11, XRS2*), chromosome segregation (e.g., *BFA1, MAD1, CIK1, KAR3*) and the DNA damage checkpoint *(PPH3*). Significantly, *DIA2* also exhibited strong interactions with a spectrum of genes that promote replication fork restart, namely *SGS1* and *TOP3*, *SLX1* and *SLX4*, *SLX5* and *SLX8*, and *MUS81* and *MMS4*; each of these gene pairs encode protein complexes that play different roles in fork restart (FABRE *et al.* 2002; FRICKE and BRILL 2003; ZHANG *et al.* 2006). In addition, *DIA2* displayed synthetic interactions with genes required for oxidative stress metabolism (e.g., *SOD1, LYS7*), transcription (e.g., *CTK1, SWI4*) and chromatin structure (e.g., *SWR1, HST4*). Recently, a cohort of systematic diploid synthetic lethal analysis by microarray (dSLAM) screens focused on DNA replication and chromosome segregation pathways recovered 112 synthetic lethal/synthetic sick interactions with a *dia2Δ* query strain, and an additional nine *dia2Δ* interactions with other query strains (PAN *et al.* 2006). Of the 55 confirmed hits in our *dia2Δ* screen, only 23 overlapped with the Pan et al dataset, indicating that neither experimental approach exhaustively identified *dia2Δ* genetic interactions. The myriad interactions recovered by each systematic *dia2Δ* screen suggested that Dia2 function is required to cope with a host of defects in normal replication, repair and recombination processes, as caused either directly or indirectly by various mutations.

Genes that perform related functions tend to cluster together in genome-wide synthetic lethal interaction profiles (TONG *et al.* 2004). We therefore performed two dimensional hierarchical clustering of the *dia2Δ* genetic interaction profile in the context of a large combined dataset of 10,334 synthetic lethal interactions (Figure 3A), as derived from 284 systematic SGA and dSLAM screens reported in the primary literature

(TONG *et al.* 2004; PAN *et al.* 2006; REGULY *et al.* 2006). As revealed by the dominant central cluster, many of the systematic screens carried out to date have focused on DNA replication, DNA damage and chromosome segregation pathways (TONG *et al.* 2004; PAN *et al.* 2006). Within this large dataset, the *dia2Δ* profile clustered most closely with query mutations that disrupt aspects of DNA replication and repair, namely homologous recombination (*rad51Δ*, *rad52Δ*, *rad54Δ*, *rad57Δ*, *hpr5Δ/srs2Δ*), the replication checkpoint (*csm3Δ*, *tof1Δ*, *mrc1Δ*), an alternative RFC complex implicated in establishment of sister chromatin cohesion (*dcc1Δ*, *ctf8Δ*, *ctf18Δ*), the MRX complex that mediates the DNA damage response and facilitates DSB repair (*mre11Δ*, *rad50Δ*, *xrs2Δ*), and post-replicative repair (*rad5Δ*, *rad18Δ*). Overall, the correlated genetic profiles revealed by hierarchical clustering suggested a role for Dia2 in some aspect of DNA replication.

In addition to the above well characterized replication and repair functions, *dia2Δ* clustered immediately adjacent to *rtt101Δ*, *rtt107Δ*/*esc4Δ* and *mms1Δ/rtt108Δ* (Figure 3A, red bar). The *RTT* genes were isolated in a screen for regulators of Ty1 transposition, which uncovered many pathways that dictate genome stability (SCHOLES *et al.* 2001). Rtt101 is the cullin subunit of an SCF-like ubiquitin ligase that has recently been implicated in replication fork progression through natural pause sites and damaged DNA (LUKE *et al.* 2006); Rtt107/Esc4 is a BRCT repeat containing protein that is required for replication restart after DNA damage (ROUSE 2004); Mms1 is required for resistance to MMS and other genotoxins (HRYCIW *et al.* 2002) and appears to operate in the same pathway as Mms22 (ARAKI *et al.* 2003). Direct inspection of all genetic interactions in this cohort revealed that 21 of 29 interactions with *rtt101Δ*, 34 of 55 hits

with *rtt107Δ* and 38 of 49 hits with *mms1Δ* also interact with *dia2Δ*; in addition, many other cross interactions were evident, including all possible pair-wise synthetic lethal interactions (Figure 3B). These similar genetic profiles suggest that Dia2, Rtt101, Rtt107 and Mms1 functions converge at the replication fork, particularly under adverse circumstances. Because the *dia2Δ* mutant exhibited a larger and more diverse set of interactions than other members of the cohort (Figure 3B), Dia2 likely performs additional functions as well.

Dia2 is required for resistance to some but not all DNA damaging agents: Mutations that compromise S-phase progression often cause sensitivity to DNA damaging agents or replication stress. Prompted by the synthetic genetic interactions identified in the SGA screen, we tested the sensitivity of a *dia2Δ* strain to various genotoxic agents, using appropriate checkpoint (*mec1Δ sml1Δ*), nucleotide excision repair (*rad14Δ*) and homologous recombination (*rad52Δ*) mutants as controls (Figure 4A). Plating efficiency of the *dia2Δ* strain was severely inhibited by the potent alkylating agent methyl methanesulfonate (MMS). This sensitivity to MMS was most likely due to defective SCF^{Dia2} activity because a *dia2Δ* strain bearing a version of Dia2 that lacked the F-box domain was as susceptible as the *dia2Δ* strain itself (Figure 4B). Intermediate growth inhibition was caused by 4-nitroquinolone-1-oxide (4-NQO), which forms bulky adducts that are substrates for nucleotide excision repair, and by camptothecin, a poison that traps covalent topoisomerase I/DNA intermediates. A high concentration of the replication inhibitor hydroxyurea (HU) modestly reduced the plating efficiency of a *dia2Δ* strain. The sensitivity of the *dia2Δ* mutant to MMS, HU and camptothecin has recently been reported in other studies (OHYA *et al.* 2005; KOEPP *et al.* 2006; PAN *et al.*

2006). To determine if these defects reflected a general sensitivity to DNA damage, we also tested sensitivity of the *dia2Δ* strain to UV light, which induces thymidine dimers and other photo products, and X-rays, which produce DSBs. Unlike many other replication and DNA damage response mutants, the *dia2Δ* strain was insensitive to these agents (Figure 4A). Dia2 thus does not appear to have a role in nucleotide excision repair or homologous recombination per se, but rather seems to aid in replication fork progression in the presence of certain DNA adducts.

The DNA damage checkpoint is essential in the absence of *DIA2*: As cells lacking Dia2 exhibited a pronounced S and G2/M cell cycle delay, reliance on non-essential checkpoint proteins recovered in the SGA screen and hypersensitivity to certain DNA damaging agents, we determined in further detail if the DNA damage checkpoint was necessary for viability of a *dia2Δ* strain (Figure 5). Mec1 and Rad53 are both essential proteins that transduce signals in the DNA damage checkpoint. Viability of *rad53Δ* and *mec1Δ* mutant strains, but not their checkpoint deficiencies, is rescued by deleting the ribonucleotide reductase inhibitor *SML1* (ZHAO *et al.* 1998). Triple mutants of the gentotype *dia2Δ mec1Δ sml1Δ* and *dia2Δ rad53Δ sml1-1* were inviable, indicating that Dia2 normally prevents some form of endogenous DNA damage that invokes a necessary checkpoint response.

To delineate the checkpoint pathway(s) that maintain *dia2Δ* viability, we assessed genetic interactions between *dia2Δ* and mutations in the S-phase (*mrc1Δ*) and DNA damage (*rad9Δ*, *rad24Δ*) branches of the checkpoint. Absence of the fork-associated checkpoint protein Mrc1 moderately reduced the growth rate of the *dia2Δ* mutant, whereas elimination of the checkpoint adaptor Rad9 and/or the clamp loading

factor Rad24 only slightly impaired growth rate (Figure 5A-C). Loss of both the Mrc1 and Rad9 branches results in synthetic lethality, but this lethality can be suppressed by overexpression of *RNR1* (ALCASABAS *et al.* 2001). As expected, a *mrc1Δ rad9Δ dia2Δ* triple mutant was inviable despite overexpression of *RNR1*. These results suggested that while either of the S-phase and DNA damage branches of the DNA checkpoint suffice to allow viability of the *dia2Δ* mutant, the S-phase branch is the more important of the two arms. Given that checkpoint activation is usually accompanied by a cell cycle delay, we anticipated that the accumulation of cells in G2/M in the *dia2Δ* mutant might be dependent on Mrc1 and/or Rad9/Rad24. However, abrogation of either of the main checkpoint branches failed to alter the G2/M cell cycle delay in *dia2Δ* strain, as shown by FACS analysis (Figure 5D). This delay thus either requires both arms of the checkpoint, or is mediated by an as yet uncharacterized checkpoint effector.

Interestingly, as recovered in the SGA screen, the *dia2Δ* strain also requires the phosphatase Pph3 for viability (Figure 2). Because Pph3 is required for dephosphorylation of γ-H2Ax and recovery from the checkpoint response (KEOGH *et al.* 2006), persistent DNA replication defects in *dia2Δ* cells may cause permanent checkpoint arrest in the absence of desensitization.

Dia2 prevents endogenous DNA damage in S-phase: The requirement for Mec1, Rad53 and Mrc1 for viability of the *dia2Δ* mutant and the accumulated S-phase fraction in asynchronous *dia2Δ* cultures (Figure 1D), suggested a possible S-phase progression defect in *dia2Δ* strains. We therefore assessed the kinetics of S-phase progression in synchronous cultures released from a mating pheromone-induced G1 phase arrest. While most of the *dia2Δ* population appeared to progress from G1 phase through to

G2/M phase with wild-type kinetics, a significant subpopulation accumulated in S-phase (Figure 6A). Signals that trigger the replication checkpoint result in Mec1-dependent activation of Rad53 (SANCHEZ *et al.* 1996; SUN *et al.* 1996), which can be monitored by an in situ kinase assay (ISA; (PELLICIOLI *et al.* 1999). Given that *dia2Δ* cells have a cell cycle delay, we tested whether this defect correlates with activation of Rad53 kinase activity. As expected, upon treatment of wild-type cells with 200 mM HU, Rad53 was activated, as revealed by its autophosphorylation in vitro (Figure 6B). However, in *dia2Δ* strains, Rad53 exhibited marked activation in untreated asynchronous cultures. Exposure to 200 mM HU further induced Rad53 autophosphorylation in *dia2Δ* cells, possibly because fewer cycling cells are in S-phase as compared to cultures arrested in HU. Because MMS and 4-NQO also further activated Rad53 in the *dia2Δ* strain (data not shown), Dia2 is not required for maximal activation of the checkpoint. To determine whether checkpoint activation in *dia2Δ* cells required S-phase progression, we monitored Rad53 phosphorylation in synchronous cultures by virtue of its phosphorylation-dependent mobility shift (Figure 6C). In the absence of genotoxic stress, wild-type cells passed through S into G2 without Rad53 phosphorylation. In contrast, while Rad53 was unphosphorylated in G1 phase in the *dia2Δ* strain, as cells progressed through S phase and into G2 phase, slower migrating Rad53 isoforms became apparent. This result suggested that Dia2 normally prevents endogenous DNA damage from arising in S-phase.

Despite the ability of a *dia2Δ* strain to activate Rad53 in response to HU, MMS and 4-NQO, the strain is nevertheless sensitive to MMS. To examine whether this sensitivity might result from a partially defective S-phase checkpoint, G1 phase cultures

were released into medium containing a low dose of MMS, which activates the intra-S-phase checkpoint but not the G1 DNA damage checkpoint (SIDOROVA and BREEDEN 1997). Wild-type cells required at least 210 min to complete replication in the presence of MMS, approximately 175 minutes longer than without DNA damage. In contrast, MMS-treated *dia2Δ* cells were unable to progress past mid S-phase for the duration of the 270 min experiment (Figure 6D). As checkpoint defective cells normally progress through S-phase faster than wild-type cells (PAULOVICH and HARTWELL 1995), sensitivity of the *dia2Δ* strain to MMS was not a consequence of a defective intra-S checkpoint, but rather due to an inability to recover from MMS-induced DNA damage.

The S-phase dependent activation of Rad53 suggested that *dia2Δ* cells accumulate endogenous DNA damage. This idea is also supported by the genetic result that *RAD52*-dependent DSB repair is required for viability of dia2Δ strains, (Figure 2), whereas in direct tetrad analysis, the Ku70/Ku80 non-homologous end joining (NHEJ) factors required to repair breaks in G1 phase are not required (data not shown). To directly assess the occurrence of DNA strand breaks in *dia2Δ* cells we measured the occurrence of DNA repair foci in live cells using YFP fusions to DNA damage responsive proteins (LISBY *et al.* 2001; MELO *et al.* 2001). As expected, Rad52^{YFP} foci formed at a low frequency in log phase cultures of wild-type cells. In contrast, the *dia2Δ* mutant showed a significant increase in foci formation of 2- and 4.5-fold in unbudded and budded cells, respectively (Figure 6E). A similar increase was seen both by TUNEL assay for DNA strand breaks and by a Ddc1^{YFP} damage foci reporter (data not shown). This increase in repair foci implies that DNA lesions, most likely DSBs, accumulate in *dia2Δ* cells and activate the DNA checkpoint response. The slight increase of Rad52

foci in G1 phase *dia2Δ* cells suggested an additional defect, perhaps due to incomplete repair of lesions before desensitization of the G2/M checkpoint arrest. However, we note that the extent of G1 phase damage foci in *dia2Δ* cells is modest compared to other DNA repair/checkpoint mutants, such as *rmi1Δ* (CHANG *et al.* 2005).

Dia2 ensures high fidelity chromosome segregation: We examined the *dia2Δ* phenotype by genome-wide expression profiles, which can often be used to deduce gene function (HUGHES *et al.* 2000a). The overall expression profile of the *dia2Δ* strain was highly similar to that of wild-type cells, with the notable exception of a 1.5 to 3.5 fold increase in RNR transcripts in the *dia2Δ* mutant (Figure 7A). *RNR* induction is a hallmark checkpoint response to replication stress (ELLEDGE and DAVIS 1990). In addition, several general stress responsive genes, including *XBP1* and *HSP26*, were elevated in the *dia2Δ* strain. Aside from the obvious transcriptional difference in *RNR* transcript levels, comparison of chromosome-wide mean expression levels revealed that two independent *dia2Δ* isolates, one haploid and one diploid, exhibited significantly higher levels of gene expression from *Chr I* and *Chr X*, respectively (Figure 7B). This result indicates that these *dia2Δ* isolates were aneuploid, consistent with previous detection of aneuploidy in other *dia2Δ* isolates (HUGHES *et al.* 2000b).

To directly test whether *dia2Δ* plays a role in chromosome segregation, the rate of chromosome loss was measured by a colony sectoring assay (HIETER *et al.* 1985). In this assay, cells carry a reporter chromosome fragment with the *SUP11* (ochre-suppressing tRNA) gene, which is used to compliment an *ade2-101* (ochre) mutation. Colonies that retain the test chromosome are white, whereas cells that undergo a loss event accumulate a red adenine biosynthesis intermediate. The *dia2Δ* mutation caused

a ~200-fold increase in chromosome loss rate relative to wild-type (Figure 7C). In comparison, the spindle checkpoint mutants *bub1Δ* and *bub3Δ* exhibit only a 50-fold increase in chromosome loss rate under identical conditions (WARREN *et al.* 2002). Dia2 thus plays a significant role in ensuring the fidelity of chromosome transmission, likely through suppression of replication-induced DSBs, which can lead directly to aneuploidy through mis-segregation events (KAYE *et al.* 2004).

Dia2 suppresses GCRs: DNA double strand breaks can lead to whole or partial chromosome loss (KAYE *et al.* 2004). We therefore tested if *dia2Δ* cells are prone to genomic alterations by using a mutator assay that measures the incidence of GCRs (CHEN and KOLODNER 1999). Rearrangements are detected in haploid cells by the simultaneous loss of *CAN1* and *URA3* from the left arm of *Chr V*, such that cells lacking *CAN1* and *URA3* are able to form colonies on medium containing 5-fluoro-orotic acid (5-FOA) and canavinine (can). Strikingly, deletion of *dia2Δ* in this reporter strain caused a 117-fold increase in GCR rate (Figure 8A). This rate is comparable to that reported for S-phase checkpoint mutants (MYUNG *et al.* 2001).

Three classes of rearrangements are detected by the GCR assay: interstitial deletions, non-reciprocal translocations, and partial deletions of *Chr V* with de novo telomere addition (KOLODNER *et al.* 2002). To characterize the spectrum of GCRs that occur in *dia2Δ* strains, we analyzed *Chr V* structure by pulse-field-gel electrophoresis (PFGE). Chromosomal DNA from the control parental strain and seven independent 5-FOA^r can^r *dia2Δ* isolates was resolved and probed with a *Chr V*-specific *MCM3* sequence (Figure 8B). In six of the seven *dia2Δ* GCR isolates, *MCM3* sequences migrated slightly faster than in the control lane, presumably due to a partial

chromosome deletion. In addition to these discrete chromosomal rearrangements, each *dia2Δ* strain tested retained a significant amount of chromosomal DNA in the well, suggestive of unresolved replication and recombination structures (DESANY *et al.* 1998).

Dia2 suppresses recombination at the rDNA locus: Each of the seven *dia2Δ* GCR isolates tested above had genomic rearrangements in addition to *Chr V*. In particular, we observed substantial mobility disparities between *Chr IV* and *Chr XII*, which normally co-migrate (Figure 8B). *Chr XII* harbors the rDNA locus as a tandem array of ~ 100-200 repeats (PETES 1979). The rDNA array is inherently unstable and undergoes cycles of expansion/contraction through intra- and inter- chromosomal recombination (KEIL and ROEDER 1984; KOBAYASHI *et al.* 1998). We thus tested if the observed rearrangements were due to alterations in *Chr XII*. Chromosomal DNA for five of the GCR isolates were resolved by PFGE and blotted with a *35S* rDNA probe. In the *dia2Δ* strains, a faster migrating *Chr XII* was evident, confirming that this chromosome had indeed undergone gross rearrangements (Figure 8C). Furthermore, cross-hybridizing signals were detected in the wells of these lanes, indicative of unresolved rDNA replication intermediates (DESANY *et al.* 1998).

To assess whether rearrangement of *Chr XII* in *dia2Δ* cells was a consequence of increased rDNA recombination, we measured recombination rates by scoring the loss of an rDNA *ADE2* marker (MERKER and KLEIN 2002). *dia2Δ* mutants lost *ADE2* at a rate 2.8-fold higher than that of wild-type cells (Figure 8D), an increase comparable to those reported for *hpr1Δ* (3.1-fold) and *sir2Δ* (4.8-fold) strains (MERKER and KLEIN 2002), both of which have defects in rDNA repeat maintenance. Consistently, the rDNA hyper-recombination phenotype in *dia2Δ* cells correlated with an accumulation of both mono-

and multimeric ERCs (Figure 8E), which are known to arise by recombination (SINCLAIR and GUARENTE 1997).

The specific defects in rDNA repeat maintenance in the *dia2Δ* mutant suggested a particularly acute role for Dia2 in this problematic region of the genome. To investigate whether Dia2 might function directly at the rDNA locus, we examined the localization of a GFP fusion protein in live cells. Dia2^{GFP} was detected in the nucleus with substantial enrichment in the nucleolus (Figure 8F). This GFP pattern was unaltered during mitosis, except for a period during late anaphase. At this stage, Dia2^{GFP} was evident in both mother and daughter nuclei with a string of fluorescence stretched across the bud neck. Because the rDNA locus has been shown to segregate later than the rest of the genome (D'AMOURS *et al.* 2004), this result demonstrates that Dia2 is tightly co-localized with the rDNA locus. Taken together, these observations suggest that Dia2 has an important, but probably not exclusive, role in maintaining rDNA integrity.

DISCUSSION

The ubiquitin system plays an important and conserved role in the control of DNA replication and the DNA damage response (BRANZEI and FOIANI 2005). Here, through characterization of the genetic and cell biological attributes of the *dia2Δ* mutant, we have uncovered a new role for the ubiquitin system in the suppression of genome instability associated with replication fork collapse. In the absence of Dia2, cells exhibit an S/G2/M cell cycle delay, greatly increased sensitivity to damage-induced replication blocks, and an increase in chromosomal lesions. As a consequence of accumulated endogenous DNA damage, the *dia2Δ* mutant constitutively activates the DNA damage

checkpoint. Activation of the checkpoint may account for the weakly invasive phenotype of the *dia2Δ* strains (KANG *et al.* 2003). The viability of *dia2Δ* strains depends on the central checkpoint kinases Mec1 and Rad53, as well as on the collective activity of factors that mediate the DNA damage and replication arms of the checkpoint (i.e., Mrc1 and Rad9). Because the pre-anaphase cell cycle delay in *dia2Δ* strains does not solely depend on Mrc1 or Rad9, it may be imposed in part by the spindle checkpoint pathway, as observed in cells treated with DNA damaging agents and a variety of replication mutants (GARBER and RINE 2002; COLLURA *et al.* 2005). Consistently, our genetic analysis indicates that viability of the *dia2Δ* strain requires full spindle function and an intact spindle assembly checkpoint. Although not recovered in our SGA screen, *dia2Δ* strains are also severely compromised in the absence of the anaphase inhibitor Pds1 (SARIN *et al.* 2004), which both mediates aspects of the DNA damage response and couples the completion of replication to the onset of mitosis (CLARKE *et al.* 1999). Despite constitutive Rad53 activation, *dia2Δ* cells exhibit highly elevated chromosome loss and GCR rates. Unrepaired replication-induced DSBs can not only cause catastrophic genome rearrangements (CHEN and KOLODNER 1999; MYUNG *et al.* 2001; KOLODNER *et al.* 2002) but can also directly lead to failures in chromosome segregation (KAYE *et al.* 2004) . Multiple aberrations in chromosome replication and segregation pathways thus appear to underlie the high rate of genome instability of the *dia2Δ* mutant.

What might be the nature of DNA damage in *dia2Δ* cells? When a replication fork stalls it may be processed into toxic replication intermediates, or alternatively, it may simply collapse, which produces DSBs (BRANZEI and FOIANI 2005). In either case, cells

accumulate repair foci, as observed in a *dia2Δ* cells. Most significantly, the genetic result that *dia2Δ* is synthetic lethal with *rad52Δ* strongly argues that DSBs accumulate in the *dia2*Δ mutant, and thus must be repaired by homologous recombination. In addition, *dia2Δ* displays synthetic genetic interactions with *sgs1Δ* and *top3Δ*, as well as with *slx4Δ*, *slx5Δ*, *slx8Δ*, *mus81Δ* and *mms4Δ*. The *SLX* genes (*SLX1,4,5,8, MUS81*, and *MMS4*) are required in the absence of the Sgs1 helicase (MULLEN *et al.* 2001), which helps resolve replication intermediates (CHANG *et al.* 2005; LIBERI *et al.* 2005; MULLEN *et al.* 2005). The Slx1/4 and Mus81/Mms4 complexes are endonucleases that cleave structures generated from stalled and collapsed forks, respectively (BASTIN-SHANOWER *et al.* 2003; FRICKE and BRILL 2003). Given its synthetic interactions with *slx* mutations, it is likely that the *dia2Δ* mutant accumulates both stalled and collapsed forks, and therefore requires the Slx products for replication restart.

In wild type cells, MMS treatment retards fork progression and inhibits late origin firing, but these effects are transient and reversed once MMS-induced damage is repaired (SANTOCANALE and DIFFLEY 1998; TERCERO and DIFFLEY 2001). In contrast, *dia2Δ* mutants completely fail to resume replication following MMS-induced DNA damage. Dia2 may thus be required for passage of replication forks through damaged DNA templates, which rapidly accumulate large protein structures as part of the repair process. The inviability of *dia2Δ sod1Δ* and *dia2Δ lys7Δ* double mutants is also consistent with a role for Dia2 in aiding replication through damaged templates, as the Sod1 superoxide dismutase and its copper chaperone Lys7 normally prevent DNA damage from endogenous oxidative stress (PAN *et al.* 2006). Because *dia2Δ* strains appear to progress through S-phase with near wild-type kinetics, it seems unlikely that

Dia2 is a component of the general replication machinery. While a significant subpopulation of a *dia2Δ* cultures are delayed for completion of S phase, this effect probably arises from checkpoint-mediated inhibition of late origins (SANTOCANALE and DIFFLEY 1998; TERCERO and DIFFLEY 2001) and/or an inability to replicate problematic regions (CHA and KLECKNER 2002; LEMOINE *et al.* 2005; ADMIRE *et al.* 2006). Consistent with this interpretation, we have been unable to detect genetic interactions between *dia2Δ* and mutant components of DNA polymerase α- primase complex encoded by *pri1-M4* or *pri2-1*, implying that Dia2 does not facilitate either replication initiation or in lagging strand DNA synthesis (data not shown).

Our systematic genetic analysis strongly suggests that Dia2 enables the replication machinery to cope with natural replication slow zones, in particular the RFB of the rDNA repeat. In budding yeast, replication pause sites occur at well defined regions throughout the genome, including the rDNA locus (ROTHSTEIN *et al.* 2000; CHA and KLECKNER 2002; IVESSA *et al.* 2002; IVESSA *et al.* 2003; TORRES *et al.* 2004a). The two related helicases Rrm3 and Pif1 have opposing effects on rDNA breakage and recombination via their ability to regulate RFB activity (IVESSA *et al.* 2000). Rrm3 suppresses fork stalling by driving fork progression through non-nucleosomal protein-DNA complexes (IVESSA *et al.* 2003; TORRES *et al.* 2004a), whereas Pif1 appears to promote fork arrest, in addition to its role in suppression of de novo telomere addition (IVESSA *et al.* 2000; PENNANEACH *et al.* 2006). The synthetic lethal interaction between *dia2Δ* and *rrm3Δ* suggests that Dia2 and Rrm3 may function redundantly to displace protein-DNA complexes, at least under some circumstances. However, because *rrm3Δ* strains are neither sensitive to DNA damaging agents nor require the Mus81/Mms4 or

Slx1/4 complexes for viability (TORRES *et al.* 2004b), Dia2 may play a more general role than Rrm3 in facilitating replication fork progression through problematic regions. Given the opposing effects of Rrm3 and Pif1 at the RFB, the synthetic lethal interaction between *dia2Δ* and *pif1Δ* is enigmatic. This interaction may reflect either the accumulation of aberrant replication-associated structures in the absence of Pif1 or, alternatively, a requirement for Pif1 in order to cope with DNA damage events that arise in the absence of Dia2. Regardless of these more general replication effects, the preferential localization of Dia2 to the nucleolus and the increased recombination at the rDNA locus in *dia2Δ* strains, as well as the synthetic lethal interactions between *dia2Δ* and both *rrm3Δ* and *pif1Δ*, clearly implicates Dia2 as a regulator of the RFB and rDNA replication.

RNA Pol II-associated protein complexes are also intrinsic barriers to replication fork progression (DESHPANDE and NEWLON 1996; AGUILERA 2002). Head-on collision between the transcriptional machinery and the replication fork results in a replication block that is resolved by Rrm3 (PRADO and AGUILERA 2005). The synthetic genetic interactions between *dia2Δ* and mutations in various elongation factors, including *ctk1Δ*, *rtf1Δ* and *cdc73Δ* (JONA *et al.* 2001; SQUAZZO *et al.* 2002), may thus be explained by an inability of the replication machinery to transit past stalled transcriptional complexes. A variety of mutations that disrupt different aspects of chromatin structure, including *hpc2Δ*, *htz1Δ*, *swr1Δ*, *chl4Δ*, *npt1Δ*, and *hst4Δ*, also exhibit synthetic genetic interactions with *dia2Δ*. Defects in chromatin architecture might engender stalled or defective transcriptional complexes that impede the replication machinery in the absence of Dia2; alternatively, chromatin remodeling may be required for recovery from intrinsic DNA

damage in the *dia2Δ* strain (VIDANES *et al.* 2005). While the *dia2Δ* mutant is defective in both telomeric and rDNA silencing (data not shown), these effects likely arise from relocalization of silencing factors to sites of endogenous DNA damage (MARTIN *et al.* 1999). Although Dia2 might conceivably regulate higher order chromatin structure and thereby indirectly affect replication and genome stability, we favor a more direct role for Dia2 in allowing the replication machinery to cope with proteinaceous barriers.

Further insight into possible *DIA2* functions comes from its overlapping genetic interactions with *RTT101*, *RTT107/ESC4* and *MMS1/RTT108*. The pair-wise synthetic lethal interactions between these four genes suggests convergence on an essential process in DNA replication. Rtt101 and Rtt107 share similar DNA damage and replication phenotypes as Dia2 (ROUSE 2004; LUKE *et al.* 2006), and both physically interact with Mms22 (HO *et al.* 2002), a protein that operates in the same pathway as Mms1 (HRYCIW *et al.* 2002; ARAKI *et al.* 2003). Intriguingly, the likely human counterpart of Rtt101, called Cul4, forms a ubiquitin ligase complex with the Ddb1 protein, and targets a variety of repair and replication associated proteins for degradation (WILLEMS *et al.* 2004). It is thus possible that Dia2 acts in a redundant fashion with an Rtt101-based ubiquitin ligase to modify or eliminate one or more substrates at the replication fork.

Two recent reports have suggested replication-associated functions for Dia2 (KOEPP *et al.* 2006; PAN *et al.* 2006). Based on apparent premature S-phase entry of synchronous cultures of a *dia2Δ* strain and detection of replication origin sequences in cross-linked Dia2 immunoprecipitates, Koepp et al proposed that Dia2 prevents precocious firing of replication origins (KOEPP *et al.* 2006). Dia2 might thus function in an

analogous manner to the CDK inhibitor Sic1, which is known to prevent Clb5/6-Cdc28 activation and subsequent origin firing (LENGRONNE and SCHWOB 2002). However, a number of our results are inconsistent with a role for Dia2 in replication initiation. We did not detect overt premature S-phase entry in the *dia2Δ* strain, at least as judged by bulk DNA replication in synchronous populations. Unlike the rescue of the *sic1Δ* phenotype by co-deletion of *clb5Δclb6Δ* (LENGRONNE and SCHWOB 2002), we did not observe amelioration of the *dia2Δ* cell size and G2/M cell cycle delay phenotypes in a *clb5Δclb6Δ* background (data not shown). Moreover, in contrast to *dia2Δ* strains, the replication checkpoint is not activated in a *sic1Δ* strain (LENGRONNE and SCHWOB 2002). The markedly different spectrum of genetic interactions exhibited by *sic1Δ* and *dia2Δ* mutations also implies different functions (in the combined dataset used to generate Figure 3A, of 153 total *dia2Δ* interactions and 62 total *sic1Δ* interactions, only 20 overlap). Finally, the inability of *dia2Δ* cells to resume replication following MMS treatment suggests a role for Dia2 beyond replication initiation.

A second recently proposed function for Dia2 is elimination of the replication- and cohesion-associated factor Ctf4 (PAN *et al.* 2006), based both on the spectrum of replication and checkpoint genes recovered with *dia2Δ* in a dSLAM genetic network (PAN *et al.* 2006), and on a putative interaction detected between Dia2 and Ctf4 in a high throughput study (HO *et al.* 2002). Consistently, overexpression of *CTF4* is toxic in wild type cells and a *cft4Δ* mutation restores viability to a *dia2Δ hst3Δ* double mutant (PAN *et al.* 2006). However, we have been unable to detect a Dia2-Ctf4 physical interaction in direct co-immunoprecipitation tests, nor does *ctf4Δ* appear to suppress the phenotype of a *dia2Δ* single mutant (data not shown). In addition, endogenous Ctf4

levels are not altered in a *dia2Δ* strain (J. Boeke and X. Pan, personal communication). The precise role of Dia2 in DNA replication thus remains a mystery.

One obvious route to understanding Dia2 function is the identification of SCF^{Dia2} substrates. While a number of interacting partners for Dia2, including Ctf4, have been reported in HTP studies (HO *et al.* 2002), to date we have been unable to convincingly recapitulate any of these physical interactions. The identification of ubiquitin ligase substrates in general remains a difficult problem. The only clear Dia2 homolog in other species is fission yeast Pof3, which like Dia2 is distinguished from other F-box proteins by the presence of both TPR and LRR repeats. The constellation of phenotypes in the *pof3Δ* mutant partially parallels that of *dia2Δ*: each accumulates DNA damage, exhibits checkpoint activation and G2/M delay and displays high chromosome loss rates (KATAYAMA *et al.* 2002). However, disparities in UV tolerance and sensitivity to microtubule-destabilizing drugs, suggest that these two F-box proteins may not have entirely analogous functions, perhaps because of divergence in checkpoint responses between budding and fission yeast (MELO and TOCZYSKI 2002). To date, no Pof3 substrates have been reported and so no further insight can be gleaned from the fission yeast homolog of Dia2. While it seems reasonable that the complex *dia2Δ* phenotype might reflect deregulation of multiple substrates, it seems likely that the primary function of Dia2 is to facilitate DNA replication through taxing regions of the genome.

Genomic regions prone to replication delays and chromosomal rearrangements have been termed replication slow zones or fragile sites (CHA and KLECKNER 2002; LEMOINE *et al.* 2005; ADMIRE *et al.* 2006). Such sites often coincide with non-nucleosomal protein-DNA complexes, as for example at rDNA repeats, tRNA genes,

telomeres and loci with high rates of transcription (IVESSA *et al.* 2003; PRADO and AGUILERA 2005). In addition, endogenous and exogenous genotoxins can burden the genome with protein-DNA complexes that arise in the course of normal repair processes. These various forms of replication impedance, when combined with defects in either the replication machinery itself or in checkpoint pathways, can lead to rampant genome instability (KOLODNER *et al.* 2002). Fragile sites in both yeast and mammalian cells are susceptible to enfeebled DNA replication and diminished checkpoint responses (RICHARDS 2001; CASPER *et al.* 2002; LEMOINE *et al.* 2005; ADMIRE *et al.* 2006). A key feature of fragile sites in yeast is persistent, and even enhanced, fragility after an initial rearrangement has occurred (ADMIRE *et al.* 2006). Moreover, many human tumors are often marked by rearrangements at common fragile site breakpoints (GLOVER and STEIN 1988; WANG *et al.* 1997). Understanding the pathways that enable the cell to cope with replication impedance at fragile regions will provide critical insight into the genesis of cancer and other genetic disorders.

ACKNOWLEDGMENTS

We thank Jef Boeke, Xuewen Pan, Grant Brown and Patrick Paddison for helpful discussions and communication of unpublished results, Rodney Rothstein, Charlie Boone, Hannah Klein and Howard Bussey for providing reagents and Nizar Batada and Jan Wildenhain for advice on data analysis. DB was supported in part by a Canadian Institutes of Health Research (CIHR) Doctoral Award. PK is a recipient of a studentship from the National Cancer Institute of Canada. DD and MT are supported by grants from the CIHR and are holders of Canada Research Chairs. MP was supported by grants

from the Swiss Federal Institute of Technology and the Swiss National Science Foundation.

LITERATURE CITED

ADMIRE, A., L. SHANKS, N. DANZL, M. WANG, U. WEIER *et al.*, 2006 Cycles of chromosome instability are associated with a fragile site and are increased by defects in DNA replication and checkpoint controls in yeast. Genes Dev **20:** 159-173.

AGUILERA, A., 2002 The connection between transcription and genomic instability. Embo J **21:** 195-201.

ALCASABAS, A. A., A. J. OSBORN, J. BACHANT, F. HU, P. J. WERLER *et al.*, 2001 Mrc1 transduces signals of DNA replication stress to activate Rad53. Nat Cell Biol **3:** 958-965.

ARAKI, Y., Y. KAWASAKI, H. SASANUMA, B. K. TYE and A. SUGINO, 2003 Budding yeast mcm10/dna43 mutant requires a novel repair pathway for viability. Genes Cells **8:** 465-480.

BAI, C., P. SEN, K. HOFMANN, L. MA, M. GOEBL *et al.*, 1996 SKP1 connects cell cycle regulators to the ubiquitin proteolysis machinery through a novel motif, the F-box. Cell **86:** 263-274.

BAO, M. Z., M. A. SCHWARTZ, G. T. CANTIN, J. R. YATES, 3RD and H. D. MADHANI, 2004 Pheromone-dependent destruction of the Tec1 transcription factor is required for MAP kinase signaling specificity in yeast. Cell **119:** 991-1000.

BASTIN-SHANOWER, S. A., W. M. FRICKE, J. R. MULLEN and S. J. BRILL, 2003 The mechanism of Mus81-Mms4 cleavage site selection distinguishes it from the homologous endonuclease Rad1-Rad10. Mol Cell Biol **23:** 3487-3496.

BRANZEI, D., and M. FOIANI, 2005 The DNA damage response during DNA replication. Curr Opin Cell Biol **17:** 568-575.

BREITKREUTZ, B. J., C. STARK and M. TYERS, 2003 Osprey: a network visualization system. Genome Biol **4:** R22.

BREWER, B. J., and W. L. FANGMAN, 1988 A replication fork barrier at the 3' end of yeast ribosomal RNA genes. Cell **55:** 637-643.

CASPER, A. M., P. NGHIEM, M. F. ARLT and T. W. GLOVER, 2002 ATR regulates fragile site stability. Cell **111:** 779-789.

CHA, R. S., and N. KLECKNER, 2002 ATR homolog Mec1 promotes fork progression, thus averting breaks in replication slow zones. Science **297:** 602-606.

CHANG, M., M. BELLAOUI, C. ZHANG, R. DESAI, P. MOROZOV *et al.*, 2005 RMI1/NCE4, a suppressor of genome instability, encodes a member of the RecQ helicase/Topo III complex. Embo J **24:** 2024-2033.

CHEN, C., and R. D. KOLODNER, 1999 Gross chromosomal rearrangements in Saccharomyces cerevisiae replication and recombination defective mutants. Nat Genet **23:** 81-85.

CHOU, S., L. HUANG and H. LIU, 2004 Fus3-regulated Tec1 degradation through SCFCdc4 determines MAPK signaling specificity during mating in yeast. Cell **119:** 981-990.

CHRISTMAN, M. F., F. S. DIETRICH and G. R. FINK, 1988 Mitotic recombination in the rDNA of S. cerevisiae is suppressed by the combined action of DNA topoisomerases I and II. Cell **55:** 413-425.

CLARKE, D. J., M. SEGAL, G. MONDESERT and S. I. REED, 1999 The Pds1 anaphase

inhibitor and Mec1 kinase define distinct checkpoints coupling S phase with mitosis in budding yeast. Curr Biol **9:** 365-368.

COLLURA, A., J. BLAISONNEAU, G. BALDACCI and S. FRANCESCONI, 2005 The fission yeast Crb2/Chk1 pathway coordinates the DNA damage and spindle checkpoint in response to replication stress induced by topoisomerase I inhibitor. Mol Cell Biol **25:** 7889-7899.

COTTA-RAMUSINO, C., D. FACHINETTI, C. LUCCA, Y. DOKSANI, M. LOPES *et al.*, 2005 Exo1 processes stalled replication forks and counteracts fork reversal in checkpoint-defective cells. Mol Cell **17:** 153-159.

D'AMOURS, D., F. STEGMEIER and A. AMON, 2004 Cdc14 and condensin control the dissolution of cohesin-independent chromosome linkages at repeated DNA. Cell **117:** 455-469.

DESANY, B. A., A. A. ALCASABAS, J. B. BACHANT and S. J. ELLEDGE, 1998 Recovery from DNA replicational stress is the essential function of the S-phase checkpoint pathway. Genes Dev **12:** 2956-2970.

DESHPANDE, A. M., and C. S. NEWLON, 1996 DNA replication fork pause sites dependent on transcription. Science **272:** 1030-1033.

EISEN, M. B., P. T. SPELLMAN, P. O. BROWN and D. BOTSTEIN, 1998 Cluster analysis and display of genome-wide expression patterns. Proc Natl Acad Sci U S A **95:** 14863-14868.

ELLEDGE, S. J., and R. W. DAVIS, 1990 Two genes differentially regulated in the cell cycle and by DNA-damaging agents encode alternative regulatory subunits of ribonucleotide reductase. Genes Dev **4:** 740-751.

FABRE, F., A. CHAN, W. D. HEYER and S. GANGLOFF, 2002 Alternate pathways involving Sgs1/Top3, Mus81/ Mms4, and Srs2 prevent formation of toxic recombination intermediates from single-stranded gaps created by DNA replication. Proc Natl Acad Sci U S A **99:** 16887-16892.

FRICKE, W. M., and S. J. BRILL, 2003 Slx1-Slx4 is a second structure-specific endonuclease functionally redundant with Sgs1-Top3. Genes Dev **17:** 1768-1778.

GARBER, P. M., and J. RINE, 2002 Overlapping roles of the spindle assembly and DNA damage checkpoints in the cell-cycle response to altered chromosomes in Saccharomyces cerevisiae. Genetics **161:** 521-534.

GIAEVER, G., A. M. CHU, L. NI, C. CONNELLY, L. RILES *et al.*, 2002 Functional profiling of the Saccharomyces cerevisiae genome. Nature **418:** 387-391.

GLOVER, T. W., and C. K. STEIN, 1988 Chromosome breakage and recombination at fragile sites. Am J Hum Genet **43:** 265-273.

GREENFEDER, S. A., and C. S. NEWLON, 1992 Replication forks pause at yeast centromeres. Mol Cell Biol **12:** 4056-4066.

HARTMAN, J. L. T., B. GARVIK and L. HARTWELL, 2001 Principles for the buffering of genetic variation. Science **291:** 1001-1004.

HERSHKO, A., 1983 Ubiquitin: roles in protein modification and breakdown. Cell **34:** 11-12.

HIETER, P., C. MANN, M. SNYDER and R. W. DAVIS, 1985 Mitotic stability of yeast chromosomes: a colony color assay that measures nondisjunction and chromosome loss. Cell **40:** 381-392.

HO, Y., A. GRUHLER, A. HEILBUT, G. D. BADER, L. MOORE *et al.*, 2002 Systematic identification of protein complexes in Saccharomyces cerevisiae by mass spectrometry. Nature **415:** 180-183.

HRYCIW, T., M. TANG, T. FONTANIE and W. XIAO, 2002 MMS1 protects against replication-dependent DNA damage in Saccharomyces cerevisiae. Mol Genet Genomics **266:** 848-857.

HUGHES, T. R., M. J. MARTON, A. R. JONES, C. J. ROBERTS, R. STOUGHTON *et al.*, 2000a Functional discovery via a compendium of expression profiles. Cell **102:** 109-126.

HUGHES, T. R., C. J. ROBERTS, H. DAI, A. R. JONES, M. R. MEYER *et al.*, 2000b Widespread aneuploidy revealed by DNA microarray expression profiling. Nat Genet **25:** 333-337.

IVESSA, A. S., B. A. LENZMEIER, J. B. BESSLER, L. K. GOUDSOUZIAN, S. L. SCHNAKENBERG *et al.*, 2003 The Saccharomyces cerevisiae helicase Rrm3p facilitates replication past nonhistone protein-DNA complexes. Mol Cell **12:** 1525-1536.

IVESSA, A. S., J. Q. ZHOU, V. P. SCHULZ, E. K. MONSON and V. A. ZAKIAN, 2002 Saccharomyces Rrm3p, a 5' to 3' DNA helicase that promotes replication fork progression through telomeric and subtelomeric DNA. Genes Dev **16:** 1383-1396.

IVESSA, A. S., J. Q. ZHOU and V. A. ZAKIAN, 2000 The Saccharomyces Pif1p DNA helicase and the highly related Rrm3p have opposite effects on replication fork progression in ribosomal DNA. Cell **100:** 479-489.

JONA, G., B. O. WITTSCHIEBEN, J. Q. SVEJSTRUP and O. GILEADI, 2001 Involvement of

yeast carboxy-terminal domain kinase I (CTDK-I) in transcription elongation in vivo. Gene **267:** 31-36.

JORGENSEN, P., I. RUPES, J. R. SHAROM, L. SCHNEPER, J. R. BROACH *et al.*, 2004 A dynamic transcriptional network communicates growth potential to ribosome synthesis and critical cell size. Genes Dev **18:** 2491-2505.

KANELLIS, P., R. AGYEI and D. DUROCHER, 2003 Elg1 forms an alternative PCNA-interacting RFC complex required to maintain genome stability. Curr Biol **13:** 1583-1595.

KANG, Z., E. WANG, L. GAO, S. LIAN, M. JIANG *et al.*, 2003 One-step water-assisted synthesis of high-quality carbon nanotubes directly from graphite. J Am Chem Soc **125:** 13652-13653.

KATAYAMA, S., K. KITAMURA, A. LEHMANN, O. NIKAIDO and T. TODA, 2002 Fission yeast F-box protein Pof3 is required for genome integrity and telomere function. Mol Biol Cell **13:** 211-224.

KAYE, J. A., J. A. MELO, S. K. CHEUNG, M. B. VAZE, J. E. HABER *et al.*, 2004 DNA breaks promote genomic instability by impeding proper chromosome segregation. Curr Biol **14:** 2096-2106.

KEIL, R. L., and G. S. ROEDER, 1984 Cis-acting, recombination-stimulating activity in a fragment of the ribosomal DNA of S. cerevisiae. Cell **39:** 377-386.

KEOGH, M. C., J. A. KIM, M. DOWNEY, J. FILLINGHAM, D. CHOWDHURY *et al.*, 2006 A phosphatase complex that dephosphorylates gammaH2AX regulates DNA damage checkpoint recovery. Nature **439:** 497-501.

KOBAYASHI, T., 2003 The replication fork barrier site forms a unique structure with Fob1p

and inhibits the replication fork. Mol Cell Biol **23:** 9178-9188.

KOBAYASHI, T., D. J. HECK, M. NOMURA and T. HORIUCHI, 1998 Expansion and contraction of ribosomal DNA repeats in Saccharomyces cerevisiae: requirement of replication fork blocking (Fob1) protein and the role of RNA polymerase I. Genes Dev **12:** 3821-3830.

KOEPP, D. M., A. C. KILE, S. SWAMINATHAN and V. RODRIGUEZ-RIVERA, 2006 The F-Box Protein Dia2 Regulates DNA Replication. Mol Biol Cell.

KOEPP, D. M., L. K. SCHAEFER, X. YE, K. KEYOMARSI, C. CHU *et al.*, 2001 Phosphorylation-dependent ubiquitination of cyclin E by the SCFFbw7 ubiquitin ligase. Science **294:** 173-177.

KOLODNER, R. D., C. D. PUTNAM and K. MYUNG, 2002 Maintenance of genome stability in Saccharomyces cerevisiae. Science **297:** 552-557.

KUS, B. M., C. E. CALDON, R. ANDORN-BROZA and A. M. EDWARDS, 2004 Functional interaction of 13 yeast SCF complexes with a set of yeast E2 enzymes in vitro. Proteins **54:** 455-467.

LAMBERT, S., A. WATSON, D. M. SHEEDY, B. MARTIN and A. M. CARR, 2005 Gross chromosomal rearrangements and elevated recombination at an inducible site-specific replication fork barrier. Cell **121:** 689-702.

LEMOINE, F. J., N. P. DEGTYAREVA, K. LOBACHEV and T. D. PETES, 2005 Chromosomal translocations in yeast induced by low levels of DNA polymerase a model for chromosome fragile sites. Cell **120:** 587-598.

LENGAUER, C., K. W. KINZLER and B. VOGELSTEIN, 1998 Genetic instabilities in human cancers. Nature **396:** 643-649.

LENGRONNE, A., and E. SCHWOB, 2002 The yeast CDK inhibitor Sic1 prevents genomic instability by promoting replication origin licensing in late G(1). Mol Cell **9:** 1067-1078.

LIBERI, G., G. MAFFIOLETTI, C. LUCCA, I. CHIOLO, A. BARYSHNIKOVA *et al.*, 2005 Rad51-dependent DNA structures accumulate at damaged replication forks in sgs1 mutants defective in the yeast ortholog of BLM RecQ helicase. Genes Dev **19:** 339-350.

LISBY, M., R. ROTHSTEIN and U. H. MORTENSEN, 2001 Rad52 forms DNA repair and recombination centers during S phase. Proc Natl Acad Sci U S A **98:** 8276-8282.

LOPES, M., C. COTTA-RAMUSINO, A. PELLICIOLI, G. LIBERI, P. PLEVANI *et al.*, 2001 The DNA replication checkpoint response stabilizes stalled replication forks. Nature **412:** 557-561.

LUKE, B., G. VERSINI, M. JACQUENOUD, I. W. ZAIDI, T. KURZ *et al.*, 2006 The cullin Rtt101 promotes replication fork progression through damaged DNA and natural pause sites. Curr Biol **16**.

MARTIN, S. G., T. LAROCHE, N. SUKA, M. GRUNSTEIN and S. M. GASSER, 1999 Relocalization of telomeric Ku and SIR proteins in response to DNA strand breaks in yeast. Cell **97:** 621-633.

MELO, J., and D. TOCZYSKI, 2002 A unified view of the DNA-damage checkpoint. Curr Opin Cell Biol **14:** 237-245.

MELO, J. A., J. COHEN and D. P. TOCZYSKI, 2001 Two checkpoint complexes are independently recruited to sites of DNA damage in vivo. Genes Dev **15:** 2809-2821.

MERKER, R. J., and H. L. KLEIN, 2002 hpr1Delta affects ribosomal DNA recombination and cell life span in Saccharomyces cerevisiae. Mol Cell Biol **22:** 421-429.

MULLEN, J. R., V. KALIRAMAN, S. S. IBRAHIM and S. J. BRILL, 2001 Requirement for three novel protein complexes in the absence of the Sgs1 DNA helicase in Saccharomyces cerevisiae. Genetics **157:** 103-118.

MULLEN, J. R., F. S. NALLASETH, Y. Q. LAN, C. E. SLAGLE and S. J. BRILL, 2005 Yeast Rmi1/Nce4 controls genome stability as a subunit of the Sgs1-Top3 complex. Mol Cell Biol **25:** 4476-4487.

MYUNG, K., A. DATTA and R. D. KOLODNER, 2001 Suppression of spontaneous chromosomal rearrangements by S phase checkpoint functions in Saccharomyces cerevisiae. Cell **104:** 397-408.

OHYA, Y., J. SESE, M. YUKAWA, F. SANO, Y. NAKATANI *et al.*, 2005 High-dimensional and large-scale phenotyping of yeast mutants. Proc Natl Acad Sci U S A **102:** 19015-19020.

PAI, K. S., D. E. BUSSIERE, F. WANG, C. A. HUTCHISON, 3RD, S. W. WHITE *et al.*, 1996 The structure and function of the replication terminator protein of Bacillus subtilis: identification of the 'winged helix' DNA-binding domain. Embo J **15:** 3164-3173.

PALECEK, S. P., A. S. PARIKH and S. J. KRON, 2000 Genetic analysis reveals that FLO11 upregulation and cell polarization independently regulate invasive growth in Saccharomyces cerevisiae. Genetics **156:** 1005-1023.

PAN, X., P. YE, D. S. YUAN, X. WANG, J. S. BADER *et al.*, 2006 A DNA Integrity Network in the Yeast Saccharomyces cerevisiae. Cell.

PATTON, E. E., A. R. WILLEMS and M. TYERS, 1998 Combinatorial control in ubiquitin-

dependent proteolysis: don't Skp the F-box hypothesis. Trends Genet **14:** 236-243.

PAULOVICH, A. G., and L. H. HARTWELL, 1995 A checkpoint regulates the rate of progression through S phase in S. cerevisiae in response to DNA damage. Cell **82:** 841-847.

PELLICIOLI, A., C. LUCCA, G. LIBERI, F. MARINI, M. LOPES *et al.*, 1999 Activation of Rad53 kinase in response to DNA damage and its effect in modulating phosphorylation of the lagging strand DNA polymerase. Embo J **18:** 6561-6572.

PENNANEACH, V., C. D. PUTNAM and R. D. KOLODNER, 2006 Chromosome healing by de novo telomere addition in Saccharomyces cerevisiae. Mol Microbiol **59:** 1357-1368.

PETES, T. D., 1979 Yeast ribosomal DNA genes are located on chromosome XII. Proc Natl Acad Sci U S A **76:** 410-414.

PICKART, C. M., 2001 Mechanisms underlying ubiquitination. Annu Rev Biochem **70:** 503-533.

PRADO, F., and A. AGUILERA, 2005 Impairment of replication fork progression mediates RNA polII transcription-associated recombination. Embo J **24:** 1267-1276.

REGULY, T., A. BREITKREUTZ, L. BOUCHER, B.-J. BREITKREUTZ, G. HON *et al.*, 2006 Comprehensive Curation and Analysis of Global Interaction Networks in *Saccharomyces cerevisiae*. J. Biol. **in press**.

RICHARDS, R. I., 2001 Fragile and unstable chromosomes in cancer: causes and consequences. Trends Genet **17:** 339-345.

ROTHSTEIN, R., B. MICHEL and S. GANGLOFF, 2000 Replication fork pausing and

recombination or "gimme a break". Genes Dev **14:** 1-10.

ROUSE, J., 2004 Esc4p, a new target of Mec1p (ATR), promotes resumption of DNA synthesis after DNA damage. Embo J **23:** 1188-1197.

SANCHEZ, Y., B. A. DESANY, W. J. JONES, Q. LIU, B. WANG *et al.*, 1996 Regulation of RAD53 by the ATM-like kinases MEC1 and TEL1 in yeast cell cycle checkpoint pathways. Science **271:** 357-360.

SANTOCANALE, C., and J. F. DIFFLEY, 1998 A Mec1- and Rad53-dependent checkpoint controls late-firing origins of DNA replication. Nature **395:** 615-618.

SARIN, S., K. E. ROSS, L. BOUCHER, Y. GREEN, M. TYERS *et al.*, 2004 Uncovering novel cell cycle players through the inactivation of securin in budding yeast. Genetics **168:** 1763-1771.

SCHOLES, D. T., M. BANERJEE, B. BOWEN and M. J. CURCIO, 2001 Multiple regulators of Ty1 transposition in Saccharomyces cerevisiae have conserved roles in genome maintenance. Genetics **159:** 1449-1465.

SIDOROVA, J. M., and L. L. BREEDEN, 1997 Rad53-dependent phosphorylation of Swi6 and down-regulation of CLN1 and CLN2 transcription occur in response to DNA damage in Saccharomyces cerevisiae. Genes Dev **11:** 3032-3045.

SINCLAIR, D. A., and L. GUARENTE, 1997 Extrachromosomal rDNA circles--a cause of aging in yeast. Cell **91:** 1033-1042.

SOGO, J. M., M. LOPES and M. FOIANI, 2002 Fork reversal and ssDNA accumulation at stalled replication forks owing to checkpoint defects. Science **297:** 599-602.

SQUAZZO, S. L., P. J. COSTA, D. L. LINDSTROM, K. E. KUMER, R. SIMIC *et al.*, 2002 The Paf1 complex physically and functionally associates with transcription elongation

factors in vivo. Embo J **21:** 1764-1774.

STARK, C., B. J. BREITKREUTZ, T. REGULY, L. BOUCHER, A. BREITKREUTZ *et al.*, 2006 BioGRID: a general repository for interaction datasets. Nucleic Acids Res **34:** D535-539.

SUN, Z., D. S. FAY, F. MARINI, M. FOIANI and D. F. STERN, 1996 Spk1/Rad53 is regulated by Mec1-dependent protein phosphorylation in DNA replication and damage checkpoint pathways. Genes Dev **10:** 395-406.

TAKEUCHI, Y., T. HORIUCHI and T. KOBAYASHI, 2003 Transcription-dependent recombination and the role of fork collision in yeast rDNA. Genes Dev **17:** 1497-1506.

TERCERO, J. A., and J. F. DIFFLEY, 2001 Regulation of DNA replication fork progression through damaged DNA by the Mec1/Rad53 checkpoint. Nature **412:** 553-557.

TERCERO, J. A., M. P. LONGHESE and J. F. DIFFLEY, 2003 A central role for DNA replication forks in checkpoint activation and response. Mol Cell **11:** 1323-1336.

TONG, A. H., M. EVANGELISTA, A. B. PARSONS, H. XU, G. D. BADER *et al.*, 2001 Systematic genetic analysis with ordered arrays of yeast deletion mutants. Science **294:** 2364-2368.

TONG, A. H., G. LESAGE, G. D. BADER, H. DING, H. XU *et al.*, 2004 Global mapping of the yeast genetic interaction network. Science **303:** 808-813.

TORRES, J. Z., J. B. BESSLER and V. A. ZAKIAN, 2004a Local chromatin structure at the ribosomal DNA causes replication fork pausing and genome instability in the absence of the S. cerevisiae DNA helicase Rrm3p. Genes Dev **18:** 498-503.

TORRES, J. Z., S. L. SCHNAKENBERG and V. A. ZAKIAN, 2004b Saccharomyces cerevisiae

Rrm3p DNA helicase promotes genome integrity by preventing replication fork stalling: viability of rrm3 cells requires the intra-S-phase checkpoint and fork restart activities. Mol Cell Biol **24:** 3198-3212.

VIDANES, G. M., C. Y. BONILLA and D. P. TOCZYSKI, 2005 Complicated tails: histone modifications and the DNA damage response. Cell **121:** 973-976.

WANG, L., W. PARADEE, C. MULLINS, R. SHRIDHAR, R. ROSATI *et al.*, 1997 Aphidicolin-induced FRA3B breakpoints cluster in two distinct regions. Genomics **41:** 485-488.

WARREN, C. D., D. M. BRADY, R. C. JOHNSTON, J. S. HANNA, K. G. HARDWICK *et al.*, 2002 Distinct chromosome segregation roles for spindle checkpoint proteins. Mol Biol Cell **13:** 3029-3041.

WILLEMS, A. R., M. SCHWAB and M. TYERS, 2004 A hitchhiker's guide to the cullin ubiquitin ligases: SCF and its kin. Biochim Biophys Acta **1695:** 133-170.

ZHANG, C., T. M. ROBERTS, J. YANG, R. DESAI and G. W. BROWN, 2006 Suppression of genomic instability by SLX5 and SLX8 in Saccharomyces cerevisiae. DNA Repair **5:** 336-346.

ZHAO, X., E. G. MULLER and R. ROTHSTEIN, 1998 A suppressor of two essential checkpoint genes identifies a novel protein that negatively affects dNTP pools. Mol Cell **2:** 329-340.

TABLE 1. Strains used in this study

Strain	Genotype	Source
YMT235	*MAT***a** *ura3-1 leu2-3,112 his3-11 15 trp1-1 ade2-1 can1-100*	K. Nasmyth
YMT1448	*MAT***a** *ura3Δ0 leu2Δ0 his3Δ1 met15Δ0*	Rosetta Inpharmatics
YMT1738	*MAT***a**/α *ura3-1/ ura3-1 leu2-3,112/ leu2-3,112 his3-11 15/ his3-11 15 trp1-1/ trp1-1 ade2-1/ ade2-1 can1-100/ can1-100 dia2Δ::HIS3/his3-11 15*	This study
YMT1817	*MAT***a** *CFIII-HIS3-SUP11 dia2Δ::URA3*	This study
YMT1819	*MAT***a** *CFIII-HIS3-SUP11*	This study
YMT1838	YMT235 *MAT***a** *dia2Δ::HIS3*	This study
YMT1874	*MAT*α *ura3-1 leu2-3,112 his3-11 15 trp1-1 ade2-1 can1-100 rad9Δ::URA3*	A. Amon
YMT1901	*MAT*α *ura3Δ0 leu2Δ0 his3Δ1 lys2Δ0 MFA1pr-HIS3 can1Δ0*	Tong et al. (2001)
YMT1940	YMT1901 *MAT*α *dia2Δ::URA3*	This study
YMT2078	*MAT***a** *ura3Δ0 leu2Δ0 his3Δ1 met15Δ0 dia2Δ : :KAN^R*	This study

YMT2084	*MAT**a** ura3-1 leu2-3,112 his3-11 15 trp1-1 ade2-1 can1-100 mec1Δ::TRP sml1Δ::HIS3*	R. Rothstein
YMT2085	*MAT**a** ura3-1 leu2-3,112 his3-11 15 trp1-1 ade2-1 can1-100 rad53Δ::HIS3 sml1-1*	R. Rothstein
YMT2545	*MAT**a** ura3-1 leu2-3,112 his3-11 15 trp1-1 ade2-1 can1-100 RDN1::ADE2 RAD5+*	H. Klein
YMT3337	*MAT**a** ura3-1 leu2-3,112 his3-11 15 trp1-1 ade2-1 can1-100* Rad52^{YFP}	R.Rothstein
YMT3398	*MAT**a** ura3-1 leu2-3,112 his3-11 15 trp1-1 ade2-1 can1-100 rad9Δ::HIS3 rad24Δ::URA3*	N. Lowndes
YMT3401	*MAT**a** ura3-1 leu2-3,112 his3-11 15 trp1-1 ade2-1 can1-100 chk1Δ::TRP rad53Δ::HIS3 sml1-1*	J.Rouse
YMT3415	*MAT**a** ura3-1 leu2-3,112 his3-11 15 trp1-1 ade2-1 can1-100* Rad52^{YFP}*, dia2Δ::TRP1*	This study
YMT3417	*MAT**a** ura3-1 leu2-3,112 his3-11 15 trp1-1 ade2-1 can1 100 mrc1Δ::NAT*	D.Durocher
YMT3420	RDKY3615 *MAT**a** ura3-52 leu2Δ1 trp1Δ63 his3Δ200 lys2-bgl hom3-10 ade2Δ1 ade8 hxt13Δ::URA3*	Chen and Kolodner (1999)
YMT3810	*MAT**a** ura3-1 leu2-3,112 his3-11 15 trp1-1 ade2-1 can1-100 RDN1::ADE2 RAD5+ dia2::KAN^R*	This study
YMT3812	RDKY3615 *MAT**a** dia2Δ::KAN^R*	This study

YMT3835	*MAT**a** ura3-1 leu2-3,112 his3-11 15 trp1-1 ade2-1 can1-100* Dia2^{GFP} (pMT3988)	This study
YMT3854	*MAT**a** ura3-1 leu2-3,112 his3-11 15 trp1-1 ade2-1 can1-100 rad9::URA3 mrc1::NAT* (pMT2581)	This study
BY4741	*MAT**a** rad14Δ::KAN^R*	EUROSCARF
BY4741	*MAT**a** rad52Δ::KAN^R*	EUROSCARF

FIGURE LEGENDS

Figure 1. The F-box protein Dia2 forms an SCF complex and is required for normal cell cycle progression. (A) Physical interactions between $Dia2^{Flag}$ and core components of the SCF complex. Cells were transformed with an empty vector or plasmids encoding $Cdc4^{FLAG}$ or $Dia2^{FLAG}$ expressed from the *GAL1* promoter, in conjunction with a CEN plasmid that expressed $Cdc53^{MYC}$ from the *CDC53* promoter. Immunoblots of whole cell lysates and anti-Flag immunoprecipitations were probed anti-Skp1 and anti-MYC antibodies. (B) Growth defect of *dia2Δ* strains. The *dia2Δ* spore clones from a sporulated heterozygous diploid *DIA2/dia2Δ* strain (yMT1738) are indicated by arrows. Cells from a representative tetrad were re-streaked onto rich medium and grown at 30^{o} for two days. (C) Cell size distribution of *dia2Δ* strains. Spore clones from a *DIA2/dia2Δ* tetrad were grown to early log phase in liquid medium, then analyzed on a Coulter Channelizer and visualized by DIC microscopy at 100x magnification. (D) DNA content of asynchronous wild-type (WT) and *dia2Δ* populations. FACS profiles were deconstructed into G1, S and G2/M components using ModFit LT software.

Figure 2. Systematic analysis of *dia2Δ* synthetic genetic interactions. A total of 55 synthetic lethal (red edges) and synthetic sick genetic interactions (black edges) detected in triplicate SGA screens were confirmed by tetrad analysis. Interactions are grouped according to indicated cellular functions and individual nodes colored by a reduced hierarchy of Gene Ontology (GO) biological processes ranked in the order shown in the color key.

Figure 3. Two-dimensional hierarchical clustering of synthetic genetic interaction profiles. (A) A combined unique set of 144 genetic interactions from *dia2Δ* query screens reported in this study and in (PAN *et al.* 2006) were clustered against 284 systematic genetic screens curated from the primary literature (REGULY *et al.* 2006). A locally dense region of interactions that contains the *dia2Δ* profile is expanded and immediate *dia2Δ* neighbors indicated by the red bar. The source of each genetic interaction is indicated by the color key. (B) Shared interactions between *dia2Δ*, *rtt101Δ*, *rtt107Δ* and *mms1Δ*. Network shows all interactions retrieved from the full 284 screen dataset for each of the four nodes. Edges are colored by interactions source; nodes are colored by the same GO biological processes as in Figure 2.

Figure 4. Dia2 is required for resistance to agents that generate DNA adducts. The indicated strains were serially diluted in 10-fold steps and plated on rich medium (A) or synthetic medium lacking tryptophan (B), either in the presence or absence of 0.02% (v/v) MMS, 200 mM HU, 5 ug/ml camptothecin, 0.1ug/ml 4-NQO, 200 J/M^2 of UV or 100 gray of X-rays . Photographs were taken after 2 days at 30°.

Figure 5. The DNA checkpoint is required for viability of a *dia2Δ* strain. (A) Representative tetrads were dissected for *dia2Δ mec1Δ sml1Δ*, *dia2Δ rad53Δ chk1Δ sml1-1*, *dia2Δ rad9Δ rad24Δ* and *dia2Δ mrc1Δ rad9Δ* heterozygous diploids. Wild-type spores are unmarked, as are inviable spores whose genotype could not be inferred. The *dia2Δ rad53Δ chk1Δ* cross carries an unmarked *sml1-1* allele to allow viability of the *rad53Δ* mutation. Note that in the last tetrad shown, *rad53Δ* alone is inviable because

sml1-1 did not segregate to this spore clone; however, specific inviability of *dia2Δ rad53Δ sml1-1* was inferred from the viability of *rad53Δ chk1Δ sml1-1* in the adjacent cross, as well as from other tetrads not shown. The *mrc1Δ rad9Δ* cross carries an <*RNR1 LEU2 2 μm*> plasmid to maintain viability of the *mrc1Δ rad9Δ* double mutant. (B) Legend for determined genotypes. (C) Summary of genetic interactions. Minus sign indicates full inviability; plus sign indicates full viability. (D) Failure of various DNA damage checkpoint mutants to bypass the G2/M cell cycle delay of *dia2Δ* strains. DNA content of asynchronous cultures of the indicated strains was determined by FACS analysis.

Figure 6. Activation of the DNA damage response in the *dia2Δ* strain. (A) Cell cycle progression of unperturbed wild-type and *dia2Δ* strains. Cells were arrested in G1 phase with alpha-factor and released into rich medium. DNA content was assessed by FACS at the indicated timepoints in minutes (B) Rad53 kinase activity was detected using an ISA assay on lysates of the indicated strains grown either in the presence or absence of 200 mM HU for one hour. Arrow indicates in situ ^{32}P incorporation into Rad53. (C) Cell cycle dependence of Rad53 activation. The indicated strains were arrested with alpha-factor and released into rich medium and lysates prepared at the indicated timepoints. Immunoblots were probed with a polyclonal Rad53 antibody. (D) Cell cycle progression of MMS-treated wild-type and *dia2Δ* strains. Cells were arrested in G1 phase with alpha-factor, released into rich medium containing 0.033% MMS and assessed for DNA content at the indicated timepoints. (E) DNA damage repair foci in a *dia2Δ* strain. Rad52^{YFP} was detected by fluorescence microscopy in wild-type and *dia2Δ*

cells. A composite of 21 collapsed Z-sections was taken for a minimum of 300 cells per strain, which were classified as unbudded (G1) and budded (S/G2/M) cells. Bars indicate standard error.

Figure 7. Dia2 is required to ensure faithful chromosome transmission. (A) Induction of *RNR* transcripts in a *dia2Δ* strain. Two replicate *dia2Δ* haploid isolates were competitively hybridized against wild-type control mRNA on genome-wide microarrays (5,989 ORFs detected) and plotted against one another. The top ten induced genes in the *dia2Δ* strain were (fold increase indicated in parentheses): *MET17(6.5x)*, *GPH1(4.2x)*, *HSP26(3.4x)*, *RNR4(2.9x)*, *YGP1(3.0x)*, *RNR2(3.4x)*, *HSP12(3.0x)*, *YMR250w(3.1x)*, *XBP1(2.3x)* and *LAP4(2.1x)*. Signals for *RNR* genes in replicate *dia2Δ* hybridizations are shown separately. (B) Aneuploidy in *dia2Δ* mutants detected by microarray analysis. Median gene induction per chromosome was calculated for independent haploid and homozygous diploid *dia2Δ* isolates. (C) Chromosome loss rates. Wild type and *dia2Δ* strains bearing an artificial test chromosome (*CFIII-SUP11-HIS3)* were plated onto non-selective media for 2 days and scored for half red/white colonies (i.e., first division mis-segregation events). At least 2,400 colonies were scored per strain.

Figure 8. Increased GCR rate is correlated with hyper-recombination at the rDNA locus in *dia2Δ* cells. (A) Assay used to detect gross chromosomal rearrangements. Sensitivity to canavinine (can) and 5-FOA selects for colonies that have undergone simultaneous loss of both genes via a GCR event. GCR rates were from two independent

experiments; fold induction was calculated as the mean of *dia2Δ* GCR rate divided by the mean GCR rate of the parental control strain. (B) Chromosomal DNA from a control and seven independent *can*^{r} *5-FOA*^{r} *dia2Δ* isolates was resolved by PFGE, stained with EtBr and probed with a chromosome V-specific *MCM3* sequence. (C) Chromsomal DNA from five of the same isolates was re-run and probed with a *35S* rDNA sequence. (D) Recombination at the rDNA locus. Wild type and *dia2Δ* strains bearing an *ADE2* marker at the rDNA locus were plated onto rich medium and grown for 3 days. Recombination rates were calculated from counting first division mis-segregation events for at least 20,000 colonies. Bars indicate standard error. (E) Accumulation of ERCs. Genomic DNA isolated from each of the indicated strains was resolved by electrophoresis and probed with rDNA sequences. Asterisk indicates chromosomal rDNA and arrows point to mono- and multi-meric ERCs (red and black arrows, respectively). (F) Sub-cellular localization of Dia2^{GFP}. A wild-type strain expressing Dia2^{GFP} was grown to log phase and visualized by fluorescence microscopy. Dia2^{GFP} signal that segregates late in anaphase as a string of fluorescence stretched across the bud neck is indicated by the arrow. Numbers in parentheses indicate percent of cells that show nucleolar Dia2 localization at each cell cycle stage.

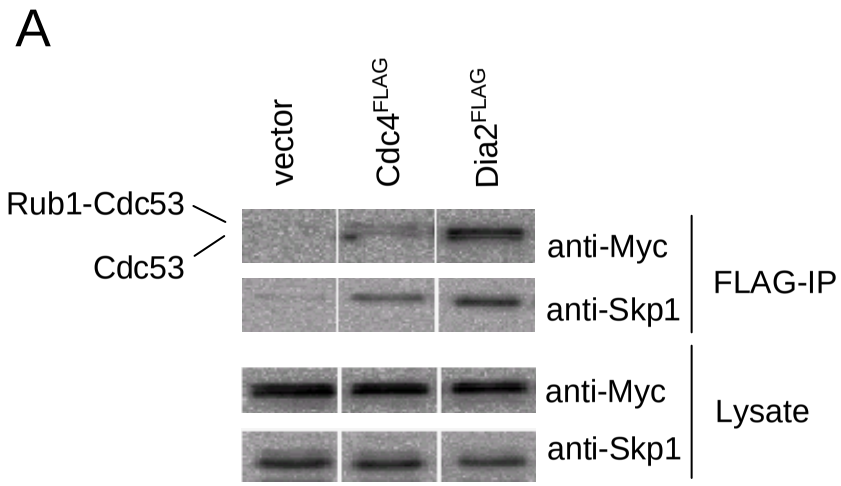

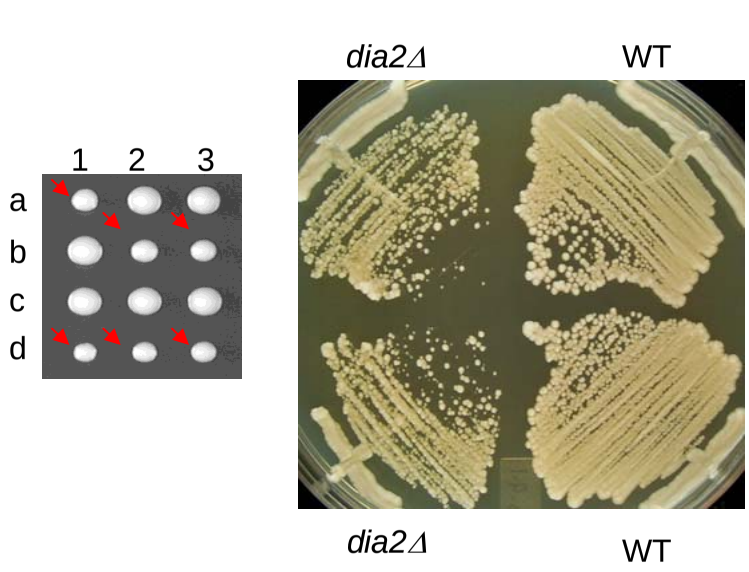

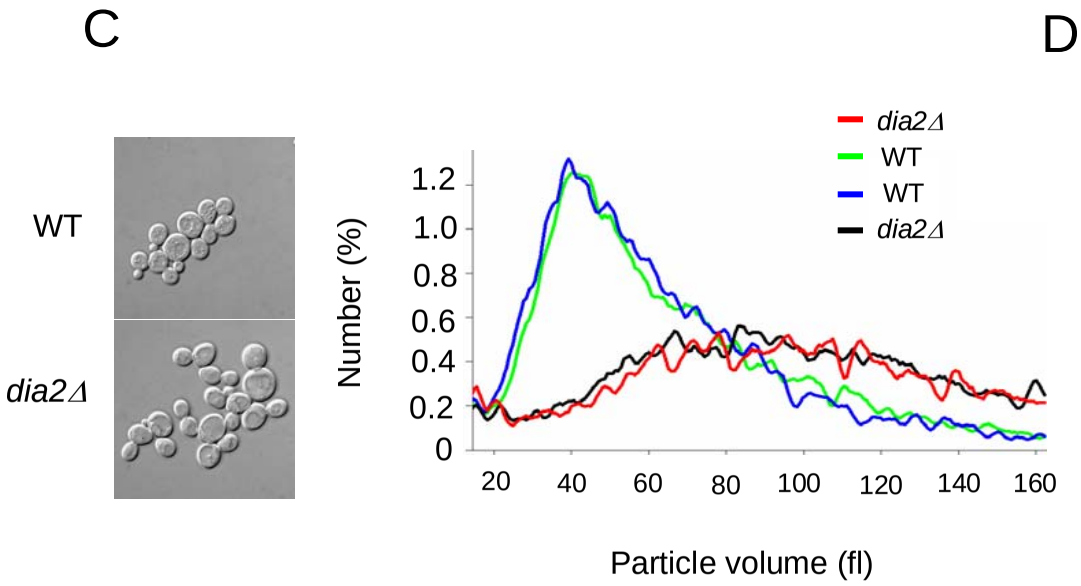

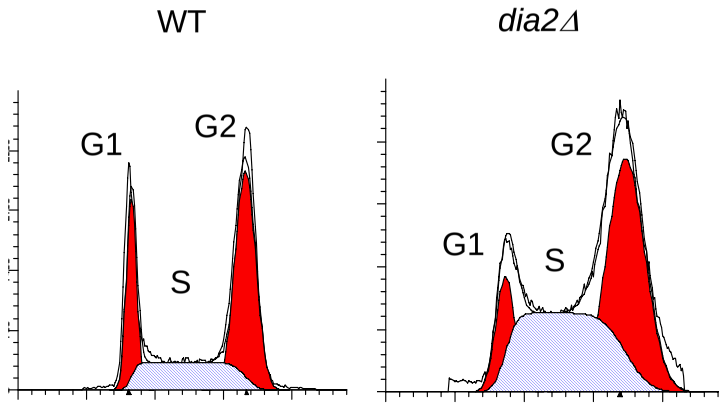

Blake et al., Fig. 1

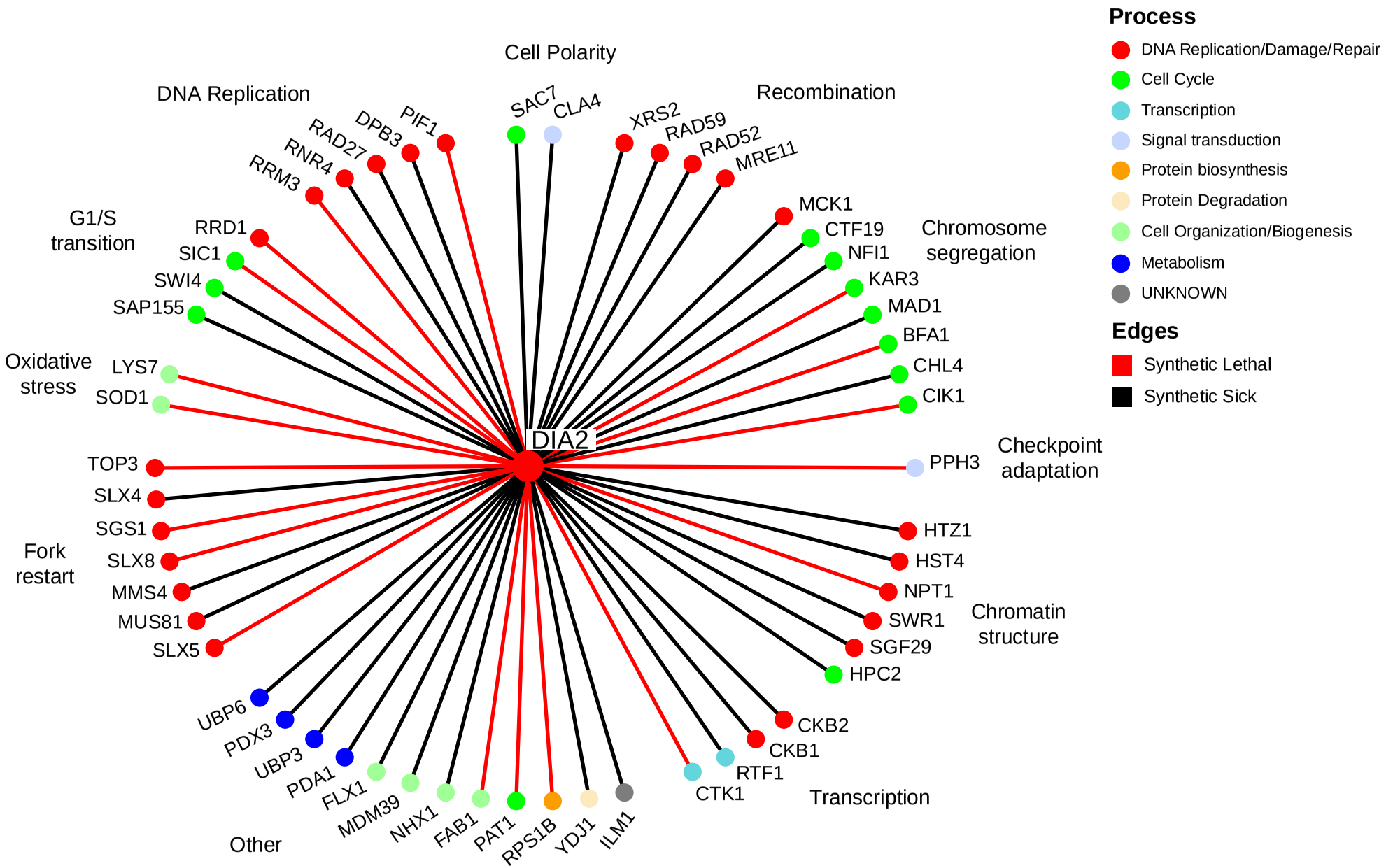

Blake et al., Fig. 2

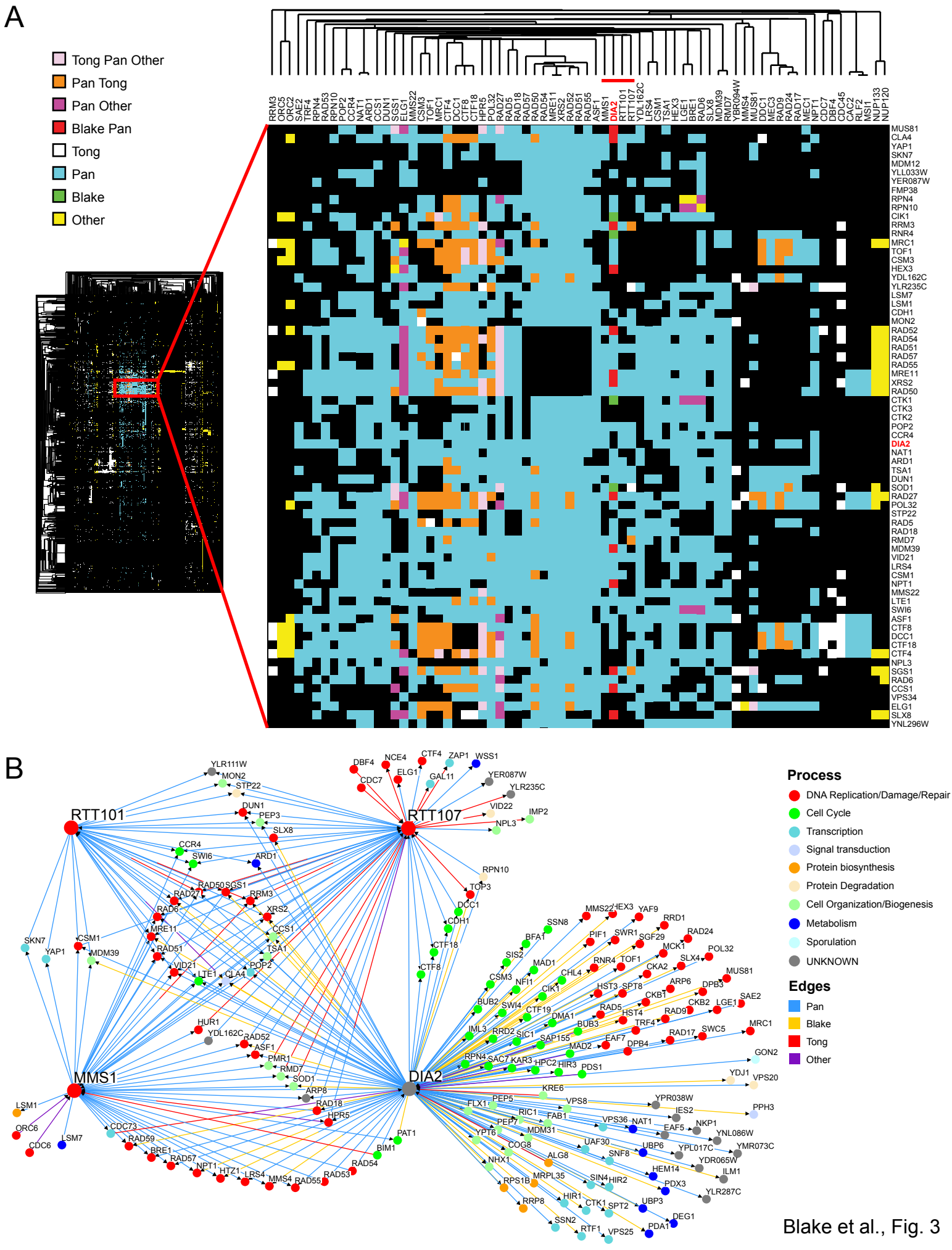

Blake et al., Fig. 3

A

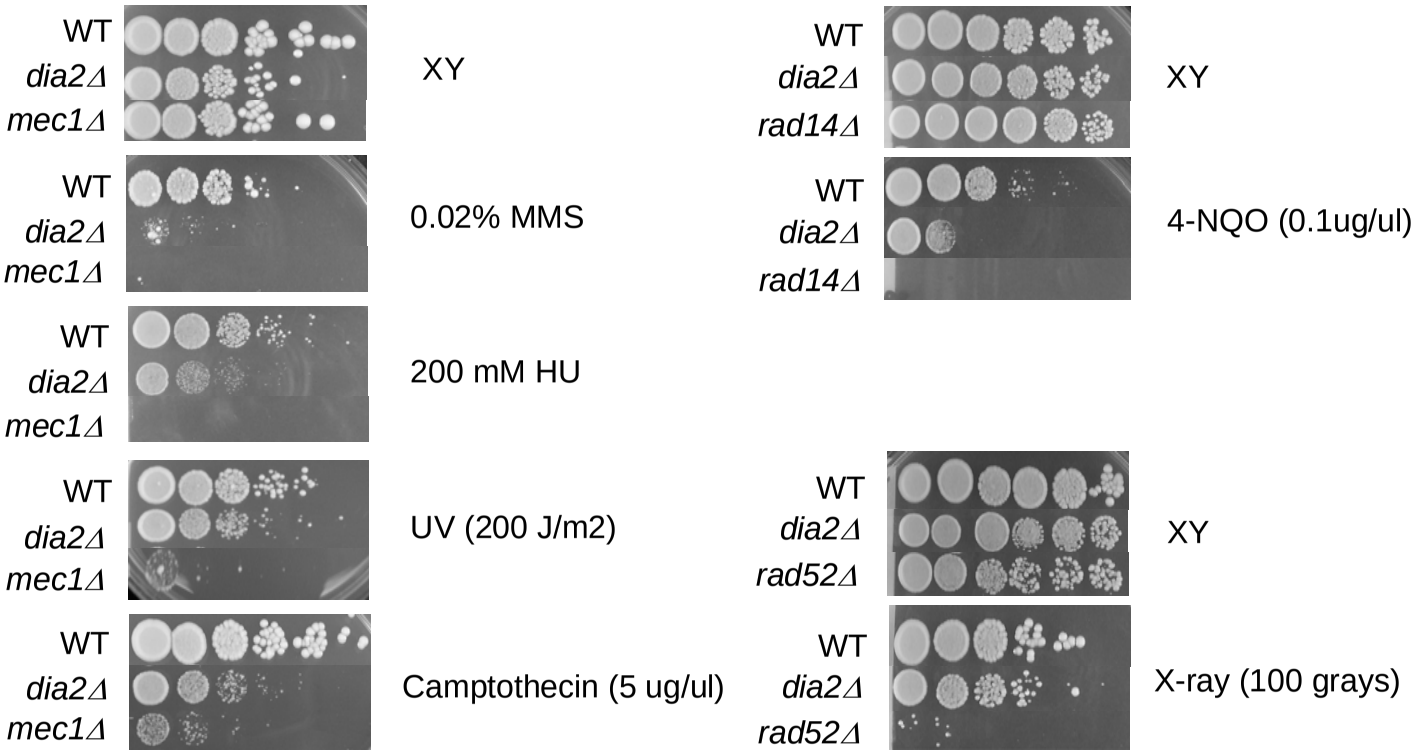

B

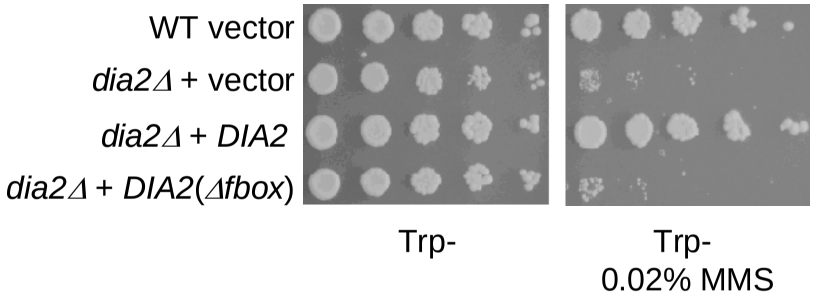

Blake et al., Fig. 4

A

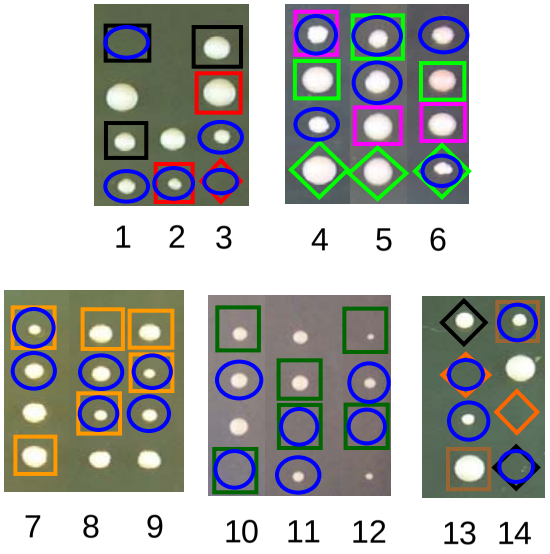

B

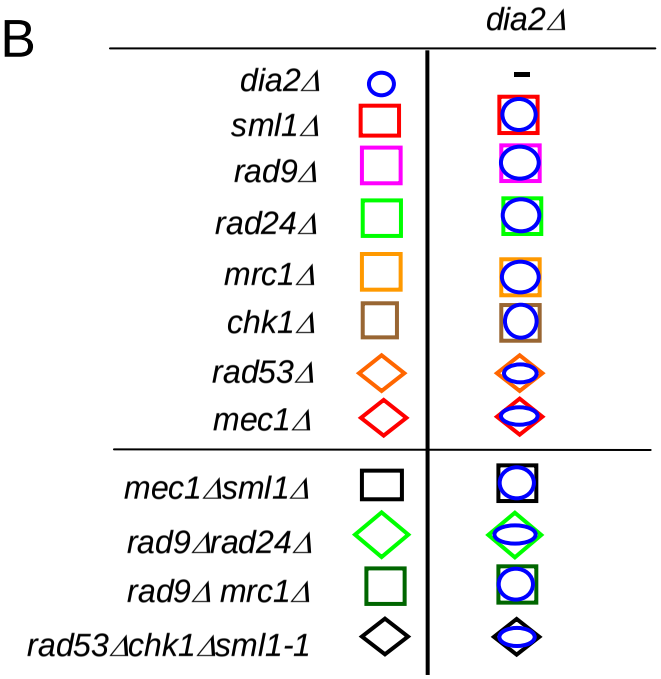

C

Function	Genotype	Viability
Checkpoint kinases	*dia2Δmec1Δsml1Δ*	-
	dia2Δsml1Δ	+
	dia2Δrad53Δchk1Δsml1-1	-
	dia2Δrad53Δsml1-1	-
DNA damage checkpoint effectors	*dia2Δrad9Δ*	+
	dia2Δrad24Δ	+/-
	dia2Δrad9Δrad24Δ	+/-
S-phase checkpoint effectors	*dia2Δmrc1Δ*	+/-
DNA damage/S-phase checkpoint	*dia2Δmrc1Δrad9Δ*	-

D

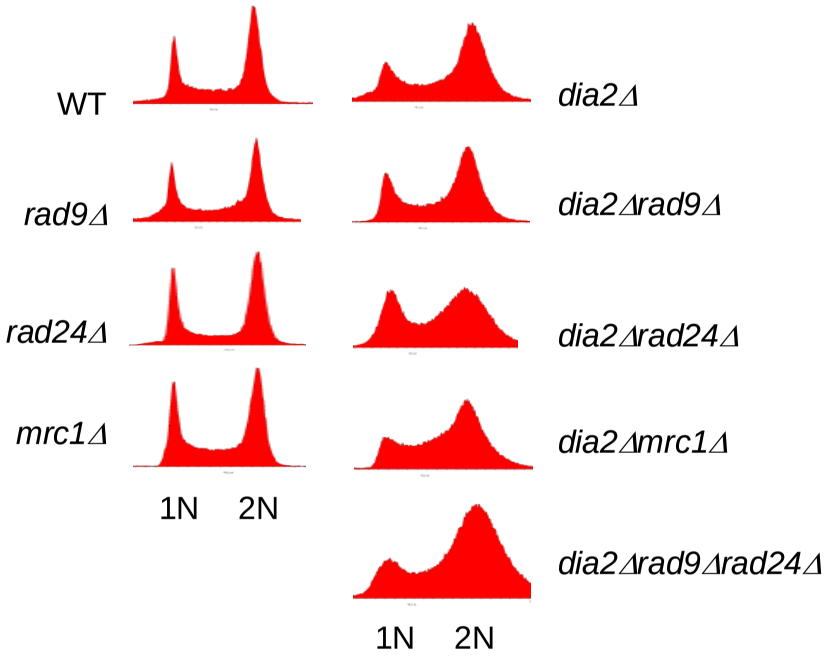

Blake et al., Fig. 5

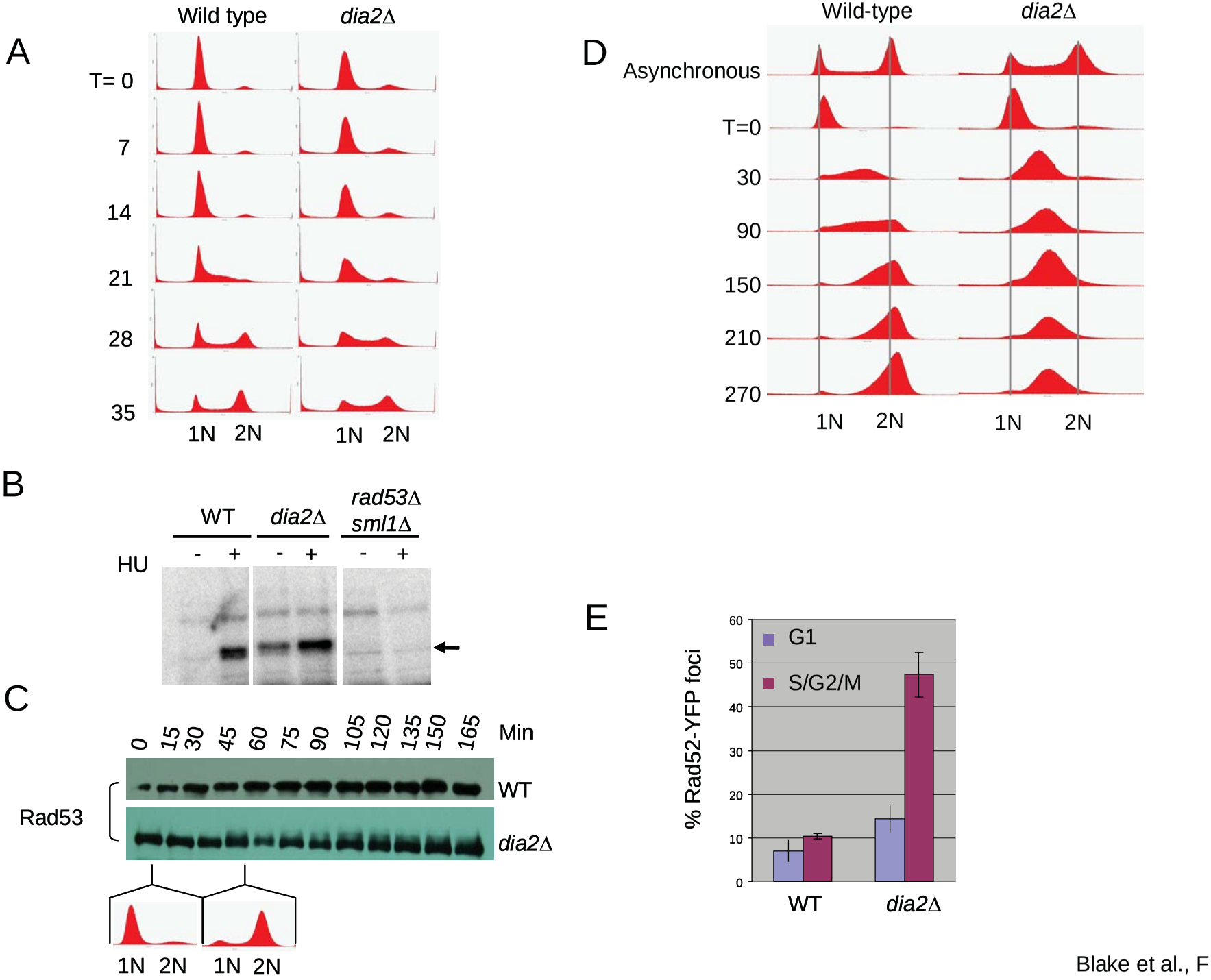

Blake et al., Fig. 6

A

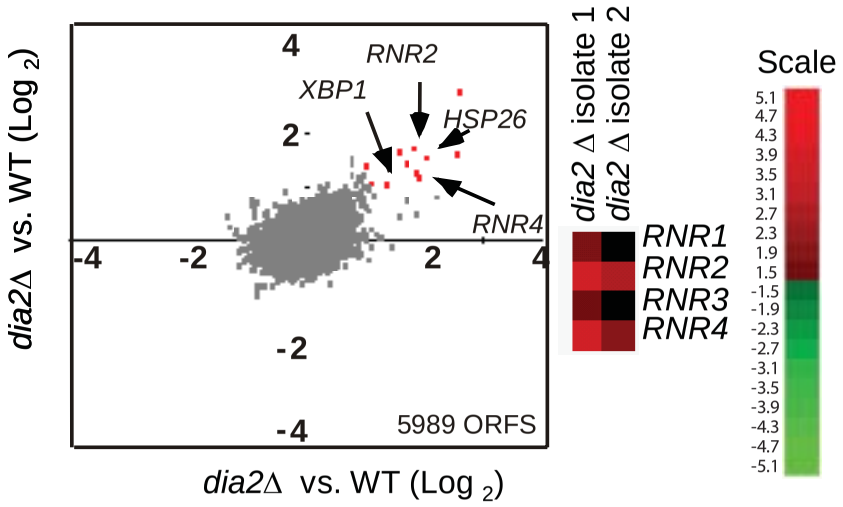

C

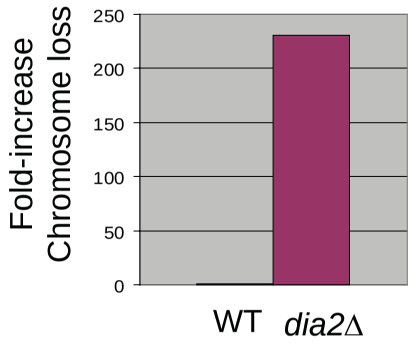

B

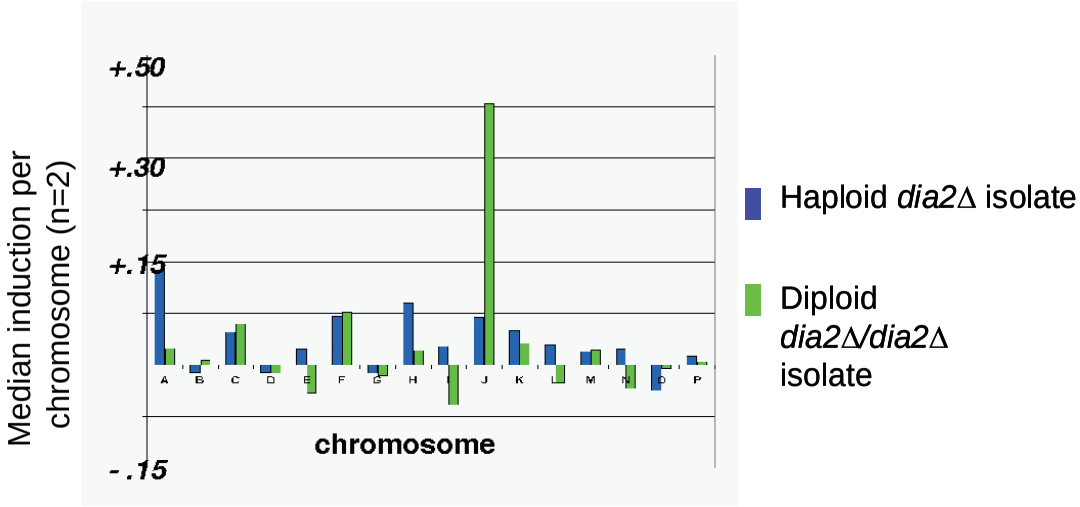

Blake et al., Fig. 7

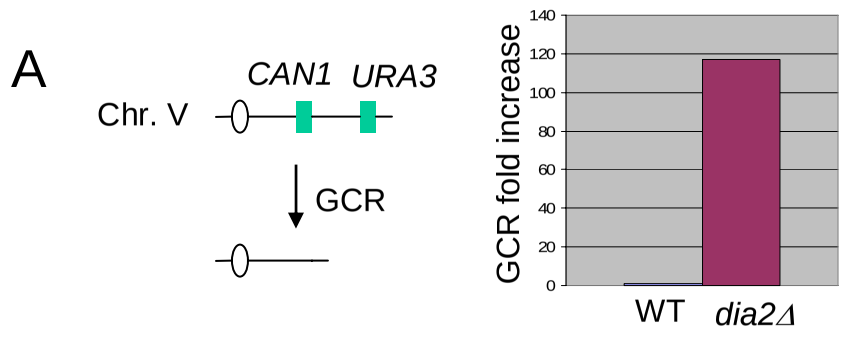

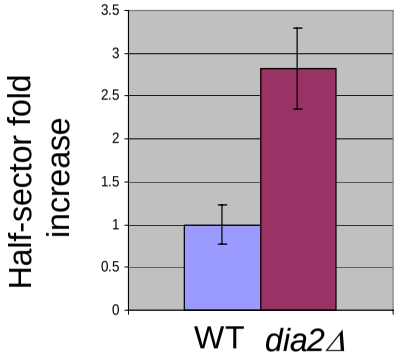

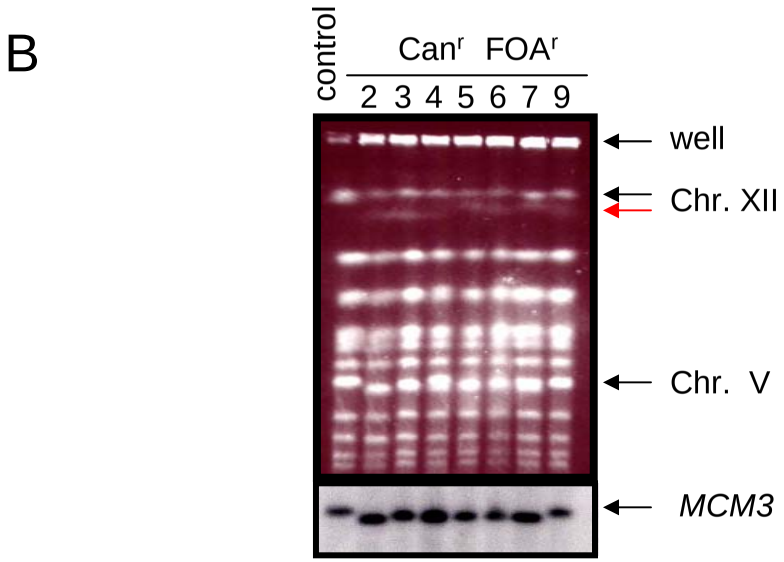

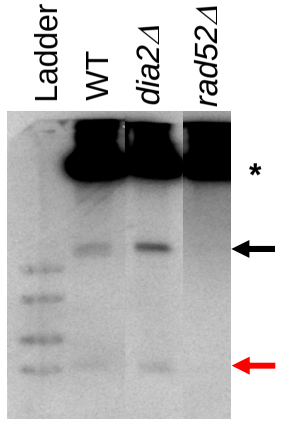

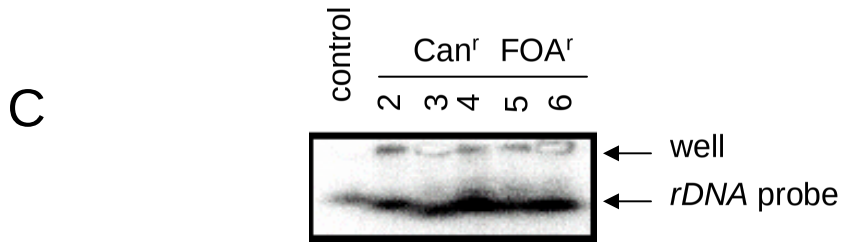

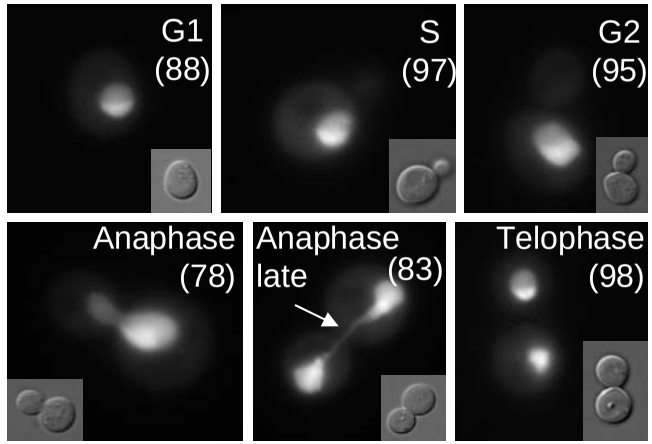

Blake et al., Fig. 8